MARMARA UNIVERSITY
INSTITUTE FOR GRADUATE STUDIES IN PURE AND APPLIED SCIENCES

DEVELOPMENT OF CMC/PEG/GO (rGO) HYDROGELS AND INVESTIGATION OF THEIR POTENTIAL USE FOR WOUND DRESSING APPLICATIONS

ÖZGE GÜLÜZAR KARACA

MASTER THESIS
Department of Chemical Engineering

Thesis Supervisor
Assoc. Prof. Neslihan Alemdar Yayla

Thesis CO- Supervisor
Assoc. Prof. Güldem Utkan

ISTANBUL, 2023

MARMARA UNIVERSITY
INSTITUTE FOR GRADUATE STUDIES
IN PURE AND APPLIED SCIENCES

DEVELOPMENT OF CMC/PEG/GO (rGO) HYDROGELS AND INVESTIGATION OF THEIR POTENTIAL USE FOR WOUND DRESSING APPLICATIONS

ÖZGE GÜLÜZAR KARACA
(524519009)

MASTER THESIS
Department of Chemical Engineering

Thesis Supervisor
Assoc. Prof. Neslihan Alemdar Yayla

Thesis CO- Supervisor
Assoc. Prof. Güldem Utkan

ISTANBUL, 2023

ACKNOWLEDGEMENT

I would like to express my sincere gratitude to my supervisors Assoc. Prof. Neslihan ALEMDAR YAYLA and Assoc. Prof. Güldem Utkan for their precious guidance and advice with this thesis. Also, I would like to thank Marmara University, Institue for Graduate Studies in Pure and Aplied Sciences, for their supports and educational conditions and Marmara University Scientific Research Project Coordination Unit (BAPKO) (Project No: FYL-2021-10283) for the financial support. Lastly, I would like to thank my family for their patience, support and encouragement throughout my educational life.

July, 2023 **Özge Gülüzar KARACA**

TABLE OF CONTENTS

PAGE

ÖZET

CMC/PEG/GO(rGO) HİDROJELLERİNİN GELİŞTİRİLMESİ VE YARA ÖRTÜ MATERYALİ UYGULAMALARI İÇİN POTANSİYEL KULLANIMLARININ ARAŞTIRILMASI

Son yıllarda, yara iyileşme sürecini etkin bir şekilde kolaylaştırması ve hızlandırması nedeniyle üstün özelliklere sahip yara örtü malzemeleri, öne çıkan bir araştırma alanıdır. İyileşme sürecini başarılı bir şekilde yönetmek için, spesifik yara koşullarına göre uygun materyali sağlamak oldukça önemlidir. Özellikle kronik yaralar, uzun süreli tedavi sonucu oluşan enfeksiyon riski nedeniyle daha fazla dikkat gerektirmektedir. Geleneksel yara örtüleri, yara iyileşmesi için ideal koşulları sağlamakta yetersiz kalırken, uygun özelliklere sahip modern yara örtüleri ile dikkat çekici sonuçlar elde edilebilmektedir. Bu nedenle, mekanik ve elektriksel özellikleri geliştirilmiş bir yara örtüsü üretebilmek için, CMC ve PEG'den oluşan bir polimerik yapıya, GO (grafen oksit) ve bitki özü (Laurus Nobilis) kullanılarak çevre dostu bir yöntemle üretilen rGO (indirgenmiş grafen oksit) ayrı ayrı katılarak yara örtü özelliklerine etkisi araştırılmış ve birbirleri ile karşılaştırılmıştır. Yapılan araştırmalar sonucunda, GO ve rGO içeren hidrojeller birbirleriyle karşılaştırıldığında, GO içeren hidrojel hidrofilik yapısı nedeniyle daha yüksek şişme oranına (%1708) ulaşırken, rGO içeren hidrojel daha kompakt yapısı nedeniyle daha az su alma kapasitesi (%605) göstermiştir. Öte yandan, hem GO hem de rGO, L-929 fibroblast hücreleri üzerinde herhangi bir toksik etki göstermemiştir. Bunun yanında, GO katkılı hidrojel %104,91'e varan canlılık değerine ulaşmış ve hücre çoğalması üzerindeki yararlı etkisini doğrulamıştır. Mekanik testler, hem GO hem de rGO'nun yapıya dahil edilmesinin, saf hidrojele kıyasla elastisite modülü, çekme mukavemeti ve kopma uzamasında önemli bir artışla sonuçlandığını göstermiştir. Saf, GO ve rGO katkılı hidrojeller arasında mekanik performans açısından en iyi sonuçlara (elastisite modülü: 588,62 N/mm^2, çekme mukavemeti: 87,99 MPa ve kopma uzaması: %17,64) rGO içeren hidrojel ulaşmıştır. Su buharı geçirgenlik sonuçlarında ise, saf hidrojel $1,5x10^{-7}$ g/Pa.h.m ile en yüksek sonucu verirken, GO ve rGO içeren hidrojeller sırasıyla $1,3x10^{-7}$ g/Pa.h.m ve $1x10^{-7}$ g/Pa.h.m değerlerini göstermiştir. Ayrıca, rGO'nun CMC bazlı hidrojelin elektriksel iletkenliğine GO'ya göre daha fazla katkı sağladığı görülmüştür. CMC/PEG/rGO-CA15% hidrojelinin iletkenlik değeri $3.01x10^{-6}$ $S.cm^{-1}$

iken, CMC/PEG/GO-CA15% hidrojelinin iletkenliği $0.85x10^{-6}$ $S.cm^{-1}$dir. Model ilaç olarak, antibiyotik içermeyen Kurkumin seçilmiş olup üretilen hidrojellerden bu ilacın salım kinetiği de incelenmiştir. Elde edilen veriler, daha az hidrofilik ve daha yoğun yapıya sahip olan rGO katkılı hidrojelin, saf ve GO katkılı hidrojele kıyasla daha kontrollü salım özelliği sağladığını göstermiştir.

Sonuç olarak, hem GO hem de rGO ile güçlendirilmiş hidrojeller, iyileştirilmiş mekanik ve iletkenlik özellikleri sayesinde yara örtü malzemeleri olarak değerlendirilebileceği saptanmıştır ve rGO katkılı hidrojelin üstün özellikleri nedeniyle yara örtüsü uygulamaları için daha uygun olabileceği gösterilmiştir.

Temmuz, 2023 **Özge Gülüzar KARACA**

ABSTRACT

DEVELOPMENT OF CMC/PEG/GO(rGO) HYDROGELS AND INVESTIGATION OF THEIR POTENTIAL USE FOR WOUND DRESSING APPLICATIONS

Recently, wound dressing materials with superior properties are an outstanding research area since they facilitate and accelerate the wound healing process in an effective way. It is vital to provide an appropriate dressing according to the specific wound conditions to successfully manage the healing process. Especially, chronic wounds require more attention due to infection risk which occurs as a result of long period of curing time. While traditional wound dressings may not be adequate in order to provide optimal wound healing conditions, modern wound dressing materials with suitable properties can achieve remarkable results. That is why, herein, in order to develop a wound dressing with enhanced electrical and mechanical features, graphene oxide (GO) and reduced graphene oxide (rGO) which is produced with environmentally friendly method by using plant extract (Laurus Nobilis) have been incorporated respectively into a polymeric structure that consists of CMC and PEG. Besides, effect of GO and rGO to the wound dressing features of the produced materials have been investigated and compared to each other. As a result of the conducted investigations, while GO containing hydrogel have reached to a higher swelling ratio (1708%) due to its hydrophilic structure, rGO containing hydrogel have shown a less water uptake capacity (605%) due to its more compact structure when compared each other. On the other hand, both GO and rGO have not shown any toxic effect on L-929 fibroblast cells. Moreover, GO reinforced hydrogel has achieved up to 104.91% viability value and confirmed its beneficial effect on cell proliferation. Mechanical tests have demonstrated that incorporation of both GO and rGO to the structure has resulted in outstanding enhancement in elongation at break, elastic modulus and tensile strength values as compared to pure hydrogel. Among pure, GO and rGO reinforced hydrogels, rGO reached to the best results in terms of mechanical performance (elastic modulus: 588.62 N/mm^2, tensile strength: 87.99 MPa and elongation at break: 17.64%). As for the water vapor permeability results, pure hydrogel showed the highest result with $1.5x10^{-7}$ g/Pa.h.m while GO and rGO reinforced hydrogels reached to $1.3x10^{-7}$ g/Pa.h.m and $1x10^{-7}$ g/Pa.h.m respectively. Besides, it was seen that rGO has made more

contribution to the electrical conductivity of the CMC based hydrogel compared to GO. While CMC/PEG/rGO-CA15% sample has $3.01x10^{-6}$ $S.cm^{-1}$ as conductivity value, the conductivity of CMC/PEG/GO-CA15% is $0.85x10^{-6}$ $S.cm^{-1}$. A model drug (Curcumin) was used for antibiotic free wound treatment and its release kinetics from the produced hydrogels was also analyzed. The results showed that rGO reinforced hydrogel having less hydrophilic and denser structure provided more controlled release feature compared to pure and GO reinforced hydrogel.

As a result, both GO and rGO reinforced hydrogels can be considered as wound dressing materials thanks to their improved mechanical and conductive properties. In other respects, it could be stated that, rGO reinforced hydrogel may be more favorable for materials used in wound dressing applications owing to its distinguished properties.

July, 2023 **Özge Gülüzar KARACA**

SYMBOLS

A	**:**	Area
C	**:**	Celsius degree
cm	**:**	Centimeter
F_{max}	**:**	Maximum force at break
h	**:**	Hour
kV	**:**	Kilovolt
µg	**:**	Microgram
µL	**:**	Microliter
mA	**:**	Milliamper
min	**:**	Minute
mL	**:**	Milliliter
mm	**:**	Milimeter
MPa	**:**	Megapascal
N	**:**	Newton
nm	**:**	Nanometer
OD	**:**	optical density
Pa	**:**	Pascal
ppm	**:**	parts per million
PV_{H2O}	**:**	saturated water vapor pressure at test temperature
RH	**:**	Relative humidity
rpm	**:**	revolutions per minute
s	**:**	slope of the curve that represents weight loss of cells versus time
t	**:**	Thickness of the film sample
V	**:**	Volt
w/w	**:**	weight per weight
W_d	**:**	Weight at dry state
W_s	**:**	Weight at swollen state
ρ	**:**	Resistance

ABBREVIATIONS

CA	**:**	Citric acid
CMC	**:**	Carboxymethyl cellulose
GO	**:**	Graphene oxide
PBS	**:**	Phosphate buffer solution
PEG	**:**	Polyethylene glycol
rGO	**:**	Reduced Graphene Oxide
RH	**:**	Relative humidity
SR	**:**	Swelling ratio
TS	**:**	Tensile Strength
WVP	**:**	Water vapor permeability

LIST OF FIGURES

PAGE

LIST OF TABLES

PAGE

1. INTRODUCTION

Skin is the largest and one of the most important organs of the body with three main layers: epidermis, dermis, and hypodermis [1]. Its fundamental purpose is to act as a protective layer to protect inner organs from microbial invasion, UV (ultraviolet) radiation and other threats. Also, its other functions are controlling body temperature, humidity and fluid loss; helping the immune and sensory systems of the body; playing an important role in homeostasis, maintaining electrolytes and nutritional components [1,4].

A wound is disintegration of the skin due to thermal/physical damage or metabolism-related issues. A wound can be acute or chronic. Acute wounds suddenly occur as a consequence of unexpected accidents such as abrasions, burns, incisions, lacerations and punctures or surgical injury. They can heal at a predictable time dependent on the severity of the injury. Burns, diabetic ulcers and leg ulcers which do not heal in a fixed time frame are examples of chronic wounds [1,5]. All type wounds, especially chronic wounds, require to be treated appropriately because they severely could affect human life and health due to infection risk [15]. The wound healing is a multi-staged and complex process which comprises of four consecutive phases: firstly, hemostasis which takes place in order to hinder over bleeding, then the inflammatory stage, after that proliferation which tissue formation and wound closure occurs and lastly remodeling phase which the skin is regenerated and tissue scar occurs [8,9,16]. Various biomolecules also participate in wound healing process such as cytokine, chemokine and growth factors. Under normal conditions, wounds can heal on their own by following these four steps. However, delayed healing can occur due to different reasons such as diabetes, a disease that affects immune system or excessive microbial burden on the wound site [8]. In these kinds of situations, advanced wound dressing materials with anti-inflammatory, antibacterial or proliferative properties are necessary to prevent bleeding and protect the wound from ambient irritants or electrolyte disturbances [3,4,9]. In order to boost the healing process, to restore the skin and to provide the best environment for wound healing, an ideal wound dressing should possess certain properties. First of all, it should mimic the natural functions of the skin. Therefore, it should not be toxic or allergenic, on the contrary, it should be biocompatible [3]. Also, it should keep the wound site moist, remove excess exudates by absorbing, provide thermal insulation, allow gas exchange, act as a barrier to

protect wound from infections and microorganisms and promote angiogenesis (growth of new blood vessels) and connective tissue synthesis. Moreover, it should be mechanically strong, easily removable from skin without causing trauma [2,4]. Recently, hydrogels have attracted great attention to be utilized as ideal wound dressings for wound healing process, since they could have all these superior features [1,6]. Hydrogels are three-dimensional macromolecular networks that comprise of chemical or physical crosslinking of vastly hydrophilic polymers [6, 7]. They can be crosslinked by physical or chemical methods. Although physical crosslinking methods for instance; ionic interactions, hydrogen bonding, Van der Waals bonds, crystallization, hydrophobic bonding, chain entanglement are better options to avoid cytotoxicity, chemical crosslinking formed by using chemical crosslinking agents could provide a better mechanical stability [6,13,14]. Hydrogels have i) highly hydrophilic nature which comes from polar functional groups within their polymer structure such as amino, amide, hydroxyl and carboxyl; ii) tissue-like structure, iii) high sensitivity to physiological environments e.g. temperature, pH and good flexibility. Additionally, not only their structures allow them to be loaded with bioactive molecules that helps wound healing and to release them to the wound site, but also they absorb excess exudates and enable oxygen diffusion to promote wound healing. Furthermore, they have water retention capacity up to several-fold of their weight allowing them to maintain the adequate moisture level at the wound site which provides cooling and soothing impact that eventually reduces the pain. [6,8]. They could also be easily removed without causing trauma thanks to their low adhesion ability. Therefore, all these excellent properties make hydrogels the most appropriate candidate to be used in wound dressing materials [7,8]. Hydrogels are mostly used on, but not limited to, burn wounds, surgical wounds, pressure ulcers (bedsores), diabetic foot ulcers, chronic leg ulcers, radiation dermatitis and these type of wounds with low to moderate exudate [8,10].

In order to boost the wound healing process, natural polymers including carboxymethyl cellulose, chitosan, alginate, collagen, hyaluronic acid etc. are mostly used in hydrogel wound dressings [9]. Among these polymers, carboxymethyl cellulose (CMC) embodies outstanding features such as high water absorption capacity, ability of gelation, biocompatibility and biodegradability which are significant properties for wound dressing applications [4].

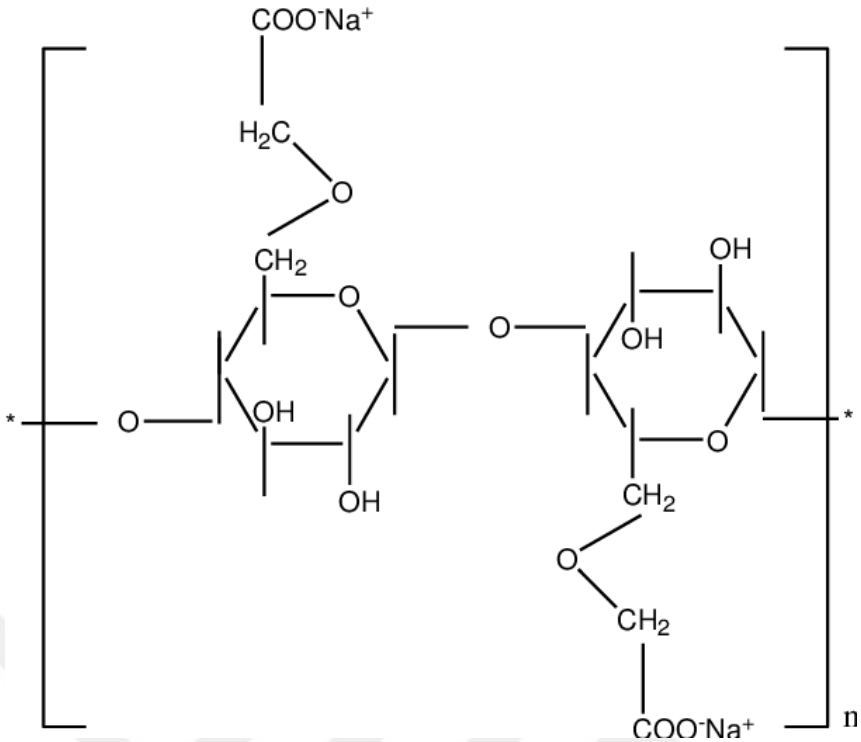

Figure 1.1: Molecular structure of the Carboxymethylcellulose (CMC) [19].

Although having most of the excellent properties to be in an ideal wound dressing material, hydrogels' drawback in this area is their inadequate mechanical stability at swollen form [6]. Mechanical stability is a very essential parameter for wound dressing materials for their practical use in biomedical applications. They should be maintaining their physical integrity and mechanical properties during the targeted application. For this purpose, several methods are used to increase mechanical performance of the hydrogel used as a wound dressing material. A composite or hybrid hydrogels that constitute two or more components are generally used to produce wound dressings with sufficient mechanical strength [6]. For this purpose, several studies have stated that polyethylene glycol (PEG) can form stable hydrogels with good mechanical and biocompatible properties. PEG which could be used in wound dressing applications thanks to its exceptional properties for instance; non-toxicity, biocompatibility, biodegradability, transparency and cost efficiency [6, 28]. Additionally, it has a water-soluble, viscous and amphiphilic structure and a good affinity for growth factors which plays a significant role in wound healing process [18]. It is also used as network modifier to improve hydrogels' properties to better pretend like natural skin [28].

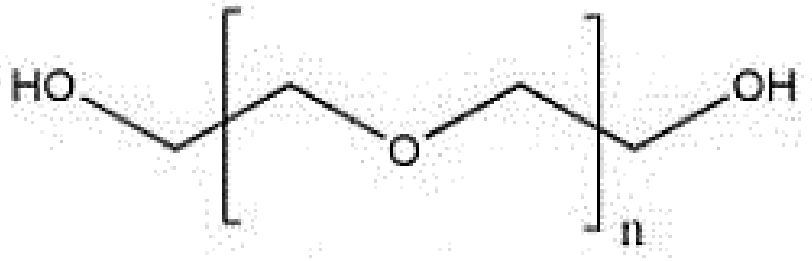

Figure 1.2: Molecular structure of the Polyethylene glycol (PEG) [30].

Another method for enhancement of mechanical performance is increasing cross-linking density. However, an optimum degree of crosslinking should be achieved when adjusting mechanical strength [11], because while increasing crosslinking density increases the physical strength, it also results in a more fragile structure by decreasing the % elongation of the hydrogel. That is why, reinforcement of polymeric structure with graphene-based materials is more effective way to increase mechanical strength of a hydrogel's structure. GO/rGO reinforced materials can achieve better results in terms of mechanical properties such as elongation at break, elastic modulus and tensile strength. For the aforementioned reasons, GO/rGO based hydrogels could be a quite favorable for wound dressing materials.

Graphene and its derivatives have attracted great attention and considered as a prominent scientific discovery due to its unique and excellent characteristic features in recent years. These features are for instance; good thermal and electrical conductivity owing to a honeycomb structure which forms sp^2 carbon structure, large surface area, intrinsic flexibility, good optical transparency along with good mechanical properties and biocompatibility [20]. Graphene oxide (GO) has a single layered structure with abundant functional groups that contain oxygen such as carboxyls, hydroxyls, and epoxides which allows for its functional modification [17]. GO has been widely utilized in biomedical applications including wound healing, biosensing, tissue engineering, drug delivery, bioimaging and gene therapy. However, it is not appropriate to use it by itself because of its potential toxicity risks albeit concentration dependent. That is why, it should be combined with other materials when applied in biomedical areas [12,17,20].

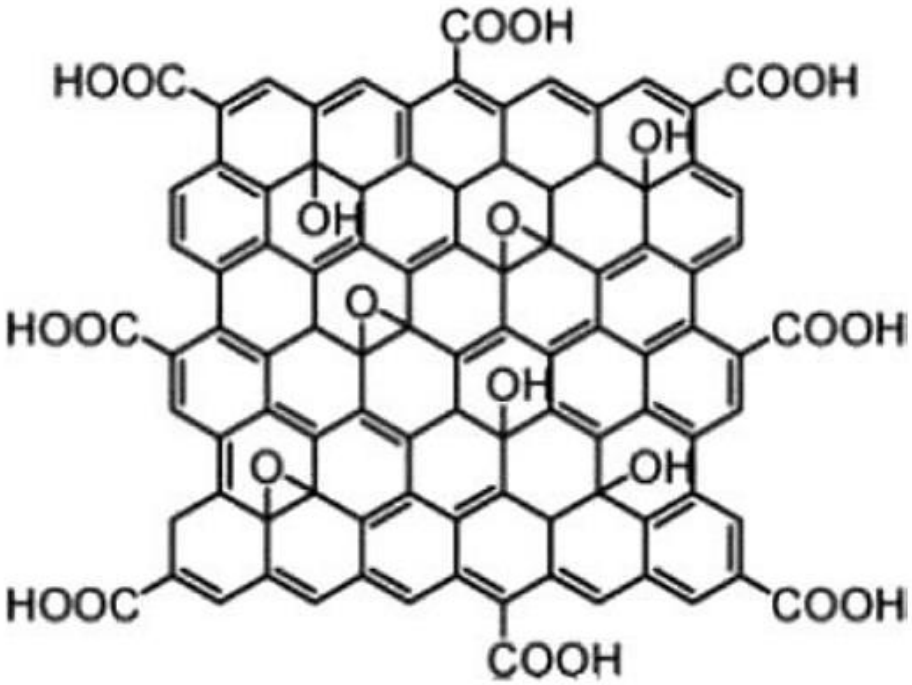

Figure 1.3: Molecular structure of the Graphene Oxide [21].

rGO is obtained through the reduction of GO. Reduction process of GO is also quite important. There are several methods to produce rGO. The method and reducing agent which are used for the reduction process are essential due to their impact on the properties (such as oxygen content or electrical and structural properties) of the final product [25]. Various reducing agents such as sodium borohydride, hydrazine and hydroquinone has been used for the reduction of GO. However, their use in biological systems may cause toxicity problems and this issue leads to a new research area for development of less hazardous reducing agents. These reducing agents can cause residual toxic by-products which also requires extra elimination process and cost. For this purpose, green reducing agents which are abundant in nature such as organic acids (e.g. ascorbic acid), sugars, plant extracts, proteins, amino acids and microorganisms have attracted attention due to their environmentally friendly features [25, 26]. Among these agents, plant extracts such as aloe vera, green tea, rosa damascena, laurus nobilis, caffeine etc. are more favorable because they provide an effective reduction owing to the molecules such as polyphenols, proteins, amino acids, vitamins etc. in their structure. These plant extracts are considered as environmentally-friendly, inexpensive and nontoxic as opposed to other chemical agents [50].

rGO differs from GO in terms of many properties i) GO is more hydrophilic and dispersible in water thanks to its oxygen containing groups while rGO is less hydrophilic [23] ii) since rGO has a larger surface area, it is mechanically stronger than GO [24], iii) a conductivity feature of rGO is far higher than that of GO because of the fact that GO's sp^2 structure which provides the conductivity is disrupted after the incorporation of oxygen containing functional groups.

When these graphene-based materials (GO or rGO) are encapsulated within the hydrogel's structure they not only enhance the mechanical strength but also provide the electrical conductivity to the structure which is important feature since conductive materials have been addressed as beneficial for wound healing as they can contribute to migration, proliferation and differentiation of electrically sensitive cells for instance; fibroblasts, keratinocytes, nerve [35]. Therefore, recently designing conductive wound dressing materials has been an impressive search. It was stated in many studies that electrical stimulation may accelerate wound healing and conductive wound dressings play an important role for this purpose. Human skin normally has a natural battery-like structure which is damaged when a wound occurs. Any damage in the skin results in a short circuit at the wound site which hinders cell migration to the wound center that contributes to wound healing. In these situations, conductive wound dressing materials could stand out to promote healing process [36, 37]. Another important topic for wound dressing research is antibiotic free applications. When the skin is damaged and cannot protect the body from environmental threads such as microorganisms and bacteria, a potential infection can lead into a chronic wound therefore affecting patients' lives [22]. Thus, it is quite important to facilitate an environment that is able to prevent bacteria and microorganism growth at the wound site. Various materials with antimicrobial activity such as antibiotics (e.g. moxifloxacin, ciprofloxacin), metal nanoparticles (e.g. Silver nanoparticles, Zinc oxide, Titanium dioxide) and natural products (e.g. essential oils, honey) are utilized for this purpose [5]. Although antimicrobial effect is generally provided with antibiotic agents, development risk of antibiotic resistance cannot be neglected. Additionally, side effects and cytotoxicity risks of antibiotics and weak penetration levels of antibiotics to the wound are also questionable. Therefore, development of antibiotic free wound dressing materials is well desired [22]. Curcumin is a good option to facilitate the desired properties in a wound dressing without using

antibiotics. Curcumin, also known as diferuloylmethane, is a natural polyphenol with outstanding bioactive properties such as anti-inflammatory, antibacterial and antioxidant activity [58]. These remarkable properties can enhance a wound dressing material when it is loaded with curcumin. It has been widely applied in biomedical science thanks to its good biocompatibility. It helps to decrease of inflammatory factors and it promotes wound healing by contributing to proliferation and maturation of phases of the wound [34].

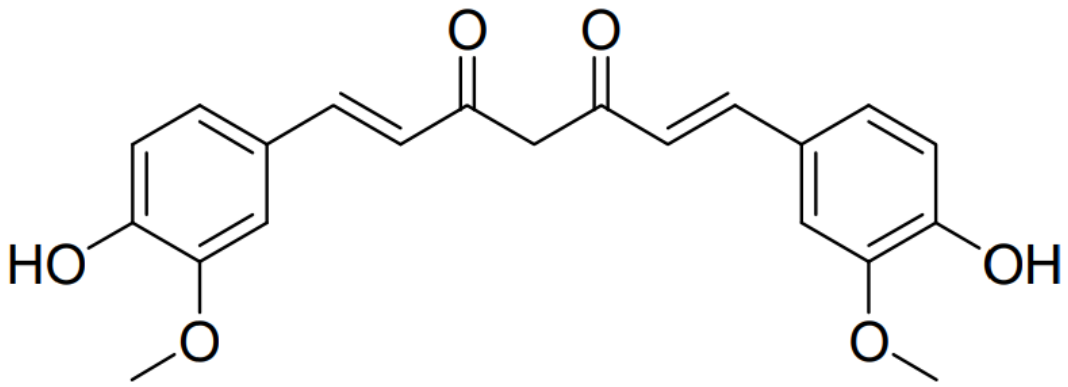

Figure 1.4: Chemical structure of the Curcumin [34]

In the light of all these information, in this study, i) CMC/PEG based wound dressing material with both improved mechanical properties and conductivity was produced through reinforcement with GO and rGO, ii) the contribution of GO and rGO to the wound dressing features have been examined and compared with each other, iii) curcumin, as a model drug, was loaded to the GO or rGO reinforced hydrogel and the release kinetic of curcumin was investigated in order to evaluate the fabricated CMC based hydrogel for antibiotic free wound dressing applications.

2. MATERIAL AND METHOD

2.1. Material

Carboxymethyl cellulose (CMC) was purchased from Sigma Aldrich (DS=0.7, Mw=250000 g/mole). Graphite powder was purchased from Syrah Resources (Australia). Polyethylene glycol (Mw=4000) was purchased from Ataman Kimya. HNO_3 was purchased from Edukim. $KMnO_4$ was purchased from Aromel Kimya. H_2O_2 was purchased from Btr Kimya. H_2SO_4 (98%) was purchased from Merck KGaA. Citric acid anhydrous (CA) was received from Ataman Kimya. Laurus nobilis was purchased from local market. Fetal Bovine Serum (FBS), Penicillin/Streptomycin, Dulbecco Modified Medium (DMEM) and Trypsin–EDTA (Trypsin–Ethylene diamine tetra acetic acid) which was used for removal of cells from culture dishes were supplied by Biological Industries. L929 (Fibroblast) cells were provided by Kırıkkale University Bioengineering Department.

2.2. Production of Graphene Oxide

GO was produced by using an adapted version of Hummer's method. Firstly, 2g of graphite powder was mixed with 5 ml HNO_3 and then 70 ml H_2SO_4 was added to the solution. After that, this solution was put in an ice bath to cool down and every 15 minutes 2g of $KMnO_4$ was slowly added to the solution for oxidation. $KMnO_4$ addition was completed at 6 times. The solution was blended for 60 minutes under room temperature. Subsequently, 100 ml of water was gradually put to the solution that was put in a water bath around 35º and the temperature increased up to 100ºC. After 10 minutes, the solution was put in an ice bath to cool down again. After 20 minutes, 300 ml of water was added to cool the solution. After 24 hours, 3 ml of H_2O_2 at 30% concentration was added at room temperature. Afterwards, the solution has been centrifuged and washed three times by deionized water. Lastly, the obtained GO was kept in oven until it was dried [29].

2.2. Production of Reduced Graphene Oxide

Laurus nobilis extract was employed for reduction of GO. The exract of Lauris nobilis was obtained by mixing 5g of Lauris nobilis leaves with 300 ml deionized water and

stirring under reflux at 90°C for 15 minutes. Subsequently, it was combined with GO solution as 1:1 (v/v) ratio and the final solution has been treated under reflux condition at 90ºC for 1 hour. Afterwards, centrifugation and washing were applied three times to the solution. Final product has been dried in oven at 40ºC [40].

2.3. Production of CMC/PEG, CMC/PEG /GO and CMC/PEG/rGO Hydrogels

Hydrogels were prepared by using CMC, PEG, GO/rGO and CA with changing amounts as shown in the table 2.1 in order to optimize the formulation of CMC based hydrogel. Firstly, CMC and PEG have been dissolved in distilled water following that CA and GO or rGO solutions within water have been added to the solution respectively in the amounts described in table 2.1. All substances were mixed at 40º for 2 hours. The final solution has been put in petri dishes and left in oven at 40ºC for 24 hours to remove the water and the formation of polymeric film. Afterwards, the samples were kept in oven at 80ºC for 8 hours for crosslinking reaction. In these formulations, while CMC and PEG were used to provide gelation, CA was employed for crosslinking. GO and rGO were used in order to improve mechanical strength and conductivity [28].

Table 2.1: Composition of produced hydrogel samples

	CMC (g)	PEG (g)	CA (g)	GO (mg)	rGO (mg)
CMC/PEG/GO - CA10%	1	0,1	0,1	3,7	-
CMC/PEG/GO-CA15%	1	0,1	0,15	3,7	-
CMC/PEG/GO-CA25%	1	0,1	0,25	3,7	-
CMC/PEG20%/GO-CA15%	1	0,2	0,15	3,7	-
CMC/PEG50%/GO-CA15%	1	0,5	0,15	3,7	-
CMC/PEG100%/GO-CA15%	1	1	0,15	3,7	-
CMC/PEG-CA15%	1	0,1	0,15	-	-
CMC/PEG/GOx4-CA15%	1	0,1	0,15	14,8	-
CMC/PEG/rGO-CA15%	1	0,1	0,15	-	3,7
CMC/PEG/rGOx4-CA15%	1	0,1	0,15	-	14,8
CMC/PEG/rGOx6,5-CA15%	1	0,1	0,15	-	24,1
CMC/PEG/rGOx26-CA15%	1	0,1	0,15	-	96,2

2.4. Characterization

Chemical structures of the graphite, GO, rGO and the produced CMC based hydrogels samples were identified by FT-IR (Fourier-transform infrared spectroscopy). Scanning of

the samples was performed between the wavenumbers of 400-4000 cm^{-1} (Perkin Elmer Spectrum Two) with attenuated total reflectance (ATR) Unit (PIKE Gladi ATR Diamond and Germanium Crystal).

Surface morphologies of the GO, rGO and CMC based hydrogels (CMC/PEG-CA15%, CMC/PEG/GO-CA15% and CMC/PEG/rGO-CA15%) have been analyzed with FE-SEM Hitachi Regulus 8230 (Field Emission Scanning Electron Microscopy). Images were acquired with 5 kV acceleration voltage. Samples were coated with 5 nm gold before examination.

2.5. Mechanical Tests

Mechanical performances of the hydrogels were determined via Zwick Roell- Z0.5 TH Mechanical Test Equipment, provided with a 0.01 N load cell. Hydrogels were cut into 1 cm x 5 cm pieces, afterwards exposed to a 2 mm/min crosshead speed and 10 mm/min load rate, at room temperature. Tensile strength (MPa), elongations at break (%) and elastic modulus (N/mm^2) of the fabricated CMC based hydrogels were assessed according to the test results. The elongation at break, tensile strength and elastic modulus values were calculated by using equations 2.1, 2.2 and 2.3.

$$TS = \frac{F_{max}}{A} \tag{2.1}$$

$$\text{Elongation at break} = (\%) = \frac{L}{L_0} * 100 \tag{2.2}$$

$$\text{Elastic modulus} = \text{stress/strain} = \frac{\frac{F}{A}}{\frac{L-L_0}{L_0}} \tag{2.3}$$

A: area of the hydrogel sample F_{max}: maximum force at rupture (N), (mm^2), L (mm): Final length of the polymeric film at break, L_0 (mm): Initial length of the polymeric film before mechanical test.

2.6. Conductivity

Conductivity tests have been conducted by using four point probe method [33]. To this end, a four point resistivity probing device (Lucas Labs S-302) was used by connecting to a Gamry Instrument power source. 0,005 mA current has been applied under 0,1 V for

5 seconds then the voltage has been doubled and continued to measurement for 5 seconds. Finally, electric current results have been recorded and conductivity values have been calculated according to the equations 2.4 and 2.5. Averages of 3 measurements have been taken for each sample.

$$\rho = \frac{\pi.t.V}{ln2.A} \quad (2.4)$$

$$\frac{1}{\rho} = \text{conductivity } \left(\frac{S}{cm}\right) \quad (2.5)$$

ρ = resistance (ohm.cm^2), t = thickness of the film sample (cm), V= voltage (Volt), A= currency (Amper)

2.7. Swelling Studies

Swelling capacity of the produced CMC based hydrogels was determined by using gravimetric method. In order to determine swelling features of the produced materials, pieces with weight around 20 mg that have been cut from hydrogels were put in falcon tubes and 20 ml of PBS (phosphate buffer solution) was added to the each one. After 24 hours of waiting, swelling ratios were determined according to the difference between dry and swollen weights of the materials (Equation 2.6).

$$\%SR = \frac{W_S - W_D}{W_D} \text{ x}100 \quad (2.6)$$

SR: Swelling ratio, W_s= Weight at swollen state, W_d= Weight at dry state

2.7. Water Vapor Permeability

Water vapor permeability (WVP) is a prominent feature for wound dressing materials. Providing an appropriate amount of humidity at the wound site is one of the key parameters of designing a wound dressing. Water vapor permeability analyses were made according to a modified version of ASTM E96 method. Each hydrogel was placed in a permeation cell that has a 0,001256 m^2 of opening area and contains anhydrous silica (0% RH) and sealed. Following that, the samples were stored at 20°C in a desiccator to provide 75% RH (relative humidity). WVP value of the samples was determined by measuring the increment in weight of the permeation cell. Cells' weights were recorded every hour

in an 8 hours period and then WVP (g H_2O Pa^{-1} s^{-1} m^{-1}) were calculated by using these recorded weight values according to the below formula (Eq. 2.7).

$$WVP = [(s/A) / (P_V{}^{H_2O}. (RH)] . d \quad (2.7)$$

Where: s =slope of the curve that represents weight loss of cells versus time (gH_2O h^{-1} m^{2}), $P_V{}^{H_2O}$ = saturated water vapor pressure (20 °C at 2339.27 Pa), RH = 0.75 (relative humidity), A = water vapor permeation area (m^2), d = hydrogel sample's thickness (m).

Each measuring for weight gain was recorded as average of three samples [32].

2.8. Cytotoxicity Tests

Cytotoxicity tests were performed consistent with the "TS EN ISO 10993-5/ MTT Cytotoxicity Test" standard. Firstly, cells were removed enzymatically (trypsin/EDTA) from culture dishes and centrifugation was applied to the cell suspension (200 g, 3 min). After that, cells were resuspended in culture media, and the suspension's cell density was modified to $10x10^3$ cells/ml. Incubation process was applied to the seeded cells for 24 hours to achieve a confluency of 80%. Following that, dilutions of the sample extract in concentration of 62.5 µg/ml were applied to the cells. Afterwards, sample extract at the appropriate concentration was added to each well, along with 100 µL of medium containing positive control, or only the medium for the negative control. Extraction was conducted according to the TS EN ISO 10993-12 standard. After incubation, a microscope was used to examine the cells in the culture dishes, culture medium of each well has been drawn. 50 µL of MTT (1 mg/ml) solution was put to each well, and the dishes were kept in the incubator for another two hours at 37 ˚C. 100 µL of isopropanol was then added to each well after the MTT solution had been removed. Without waiting, a microplate reader with a 570 nm filter (the reference wavelength is 650 nm) was used to measure absorbance.. Color changes in the plates were measured in order to calculate Viability % values at 570 nm in the spectrophotometer. The reduction in living cell number also results in a reduction in the sample's metabolic activity. The amount of formazan occred in blue-violet, which is recorded at 570 nm as optical density, is directly correlated with this reduction. The following equation is used to determine the viability decrease in comparison to the negative control value:

$$\% \text{ viability} = \frac{OD570e \times 100}{OD570b} \quad (2.8)$$

OD: optical density, e: experiment, b: blank control.

If the viability is less than 70% of the value obtained from the negative control, the test sample has cytotoxic potential.

2.9. Drug Release

For drug release studies, firstly, curcumin solution (500 ppm) has been prepared. 1:1 ethanol-water mixture has been used to ensure curcumin is completely solubilized. Then, hydrogel samples have been exposed to curcumin solution for 24 hours at 37 ºC and 130 rpm for drug loading. At the end of this period, the samples have been washed with ethanol – water (1:1) solution to remove drug molecules at the samples' surface. They were dried at room temperature and put into falcon tubes that contain 15 ml of ethanol-water solution [53]. Their drug release behaviors have been followed under 37 ºC and 130 rpm to mimic body conditions. Concentration of the media has been determined by measuring absorbance value at 430 nm periodically via UV-Vis spectrophotometry (Agilent Cary 60 Spectrophotometer). For each measurement at the end of the certain period, 3 ml of solution has been taken from the falcon tubes and the same amount of new water-ethanol solution was added to each tube. The absorbance value of the taken sample was read at 430 nm to determine the amount of delivered drug.

3. RESULTS and DISCUSSION

3.1. Characterization of graphite, GO and rGO

Graphite, GO and rGO have been characterized by FT-IR analyses. When viewed the FT-IR spectrums, it was seen that while the peak that occurs around 3400 cm^{-1} which is attributed to OH^- groups is stronger in GO due to abundance of OH^- groups, this peak gets weaker in rGO since OH^- groups are removed from the structure. Also, the peak observed at 2983 cm^{-1} that represents C-H bonds appears more intense in GO and rGO when compared to the graphite [38]. The peak that appears at 1751 cm^{-1} in Graphene oxide's spectrum is ascribed to C=O groups of carboxylic acid groups. While the intensity of the peak that occurs at 1751 cm^{-1} which refers to C=O groups of carboxylic acid groups decreases in rGO compared to GO, it completely disappears graphite's spectrum. The peak that appears at approximately1600 cm^{-1} is based upon C=C aromatic groups of the graphene skeleton [47, 39]. As the peak that observed at 1381 cm^{-1} is ascribed to the stretching band of C-OH of carboxylic acid groups is seen at a further extensive manner in GO spectrum in comparison with rGO. While the peak that occurs at 1072 cm^{-1} referring to the epoxide (C-O-C) groups is stronger in GO's spectrum, it gets more depressed in rGO and graphite's spectrum [38].

The significant declination of the intensity of all oxygen containing groups in the FT-IR spectra of rGO is clear evidence that GO has been successfully reduced by using enviromentally friendly synthesis green method in this study.

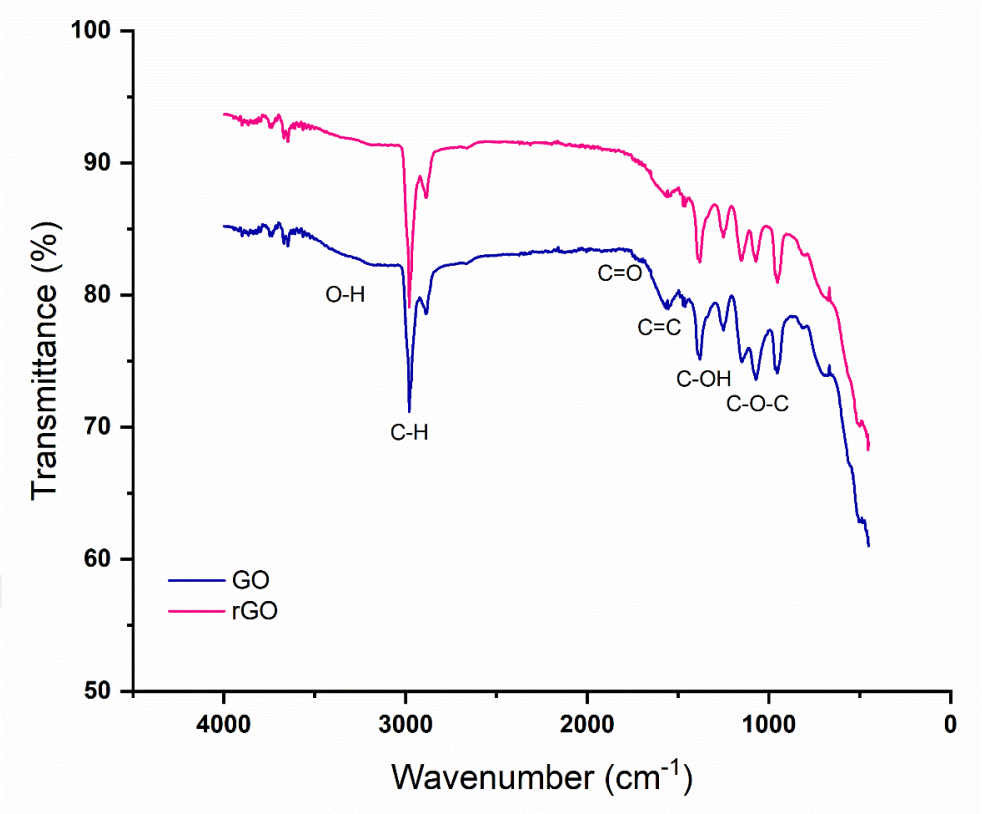

Figure 3.1: FT-IR spectrum of graphite, GO and rGO

In order to show the differences between the surface's structure of GO and rGO, the obtained SEM figures were given in figure 3.2. As seen from the figures, while GO has a more flake like texture and the interspaces between its layers are larger owing to the existence of abundant functional groups that contain oxygen, the rGO sheets get closer to each other due to reduction process and thus the interlayer spacing between graphene sheets reduces compared to GO.

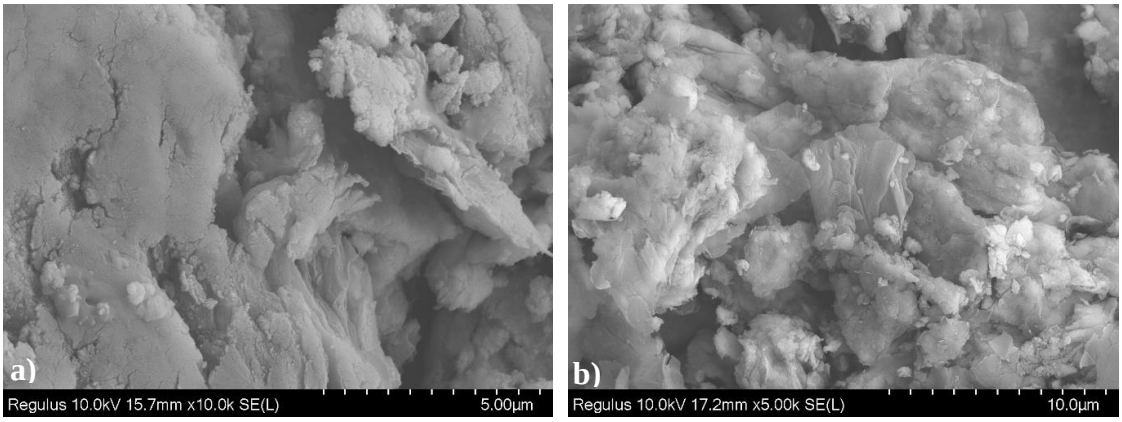

Figure 3.2: SEM figures of a) Graphen Oxide (GO), b) Reduced Graphen Oxide (rGO)

3.2. Production of CMC Based Conductive Hydrogel

CMC based conductive hydrogels were fabricated by choosing three different formulations (CMC/PEG-CA15%, CMC/PEG/GO-CA15% and CMC/PEG/rGO-CA15%) according to the swelling ratio results to evaluate as wound dressing materials (Figure 3.3).

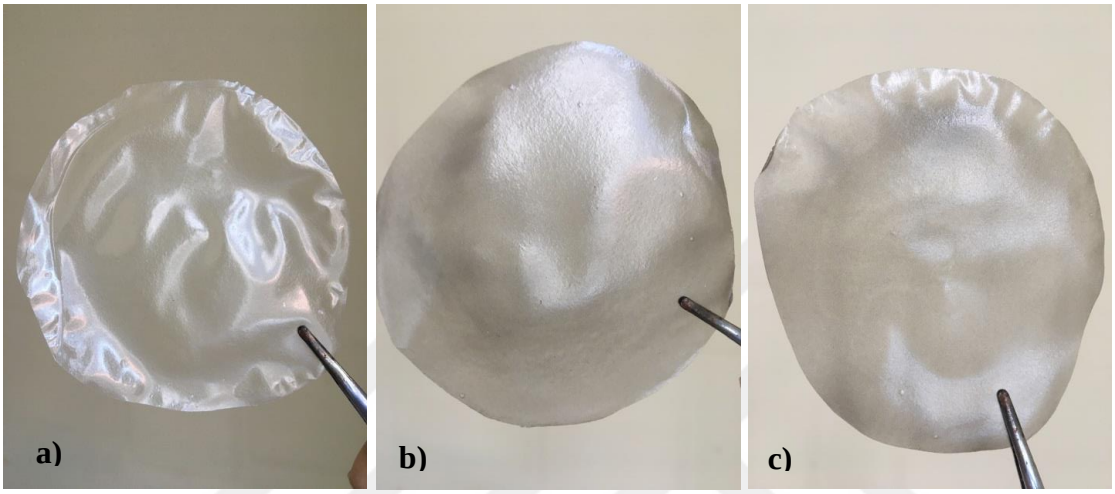

Figure 3.3: a) CMC/PEG-CA%15, b) CMC/PEG/GO-CA%15, c) CMC/PEG/rGO-CA%15

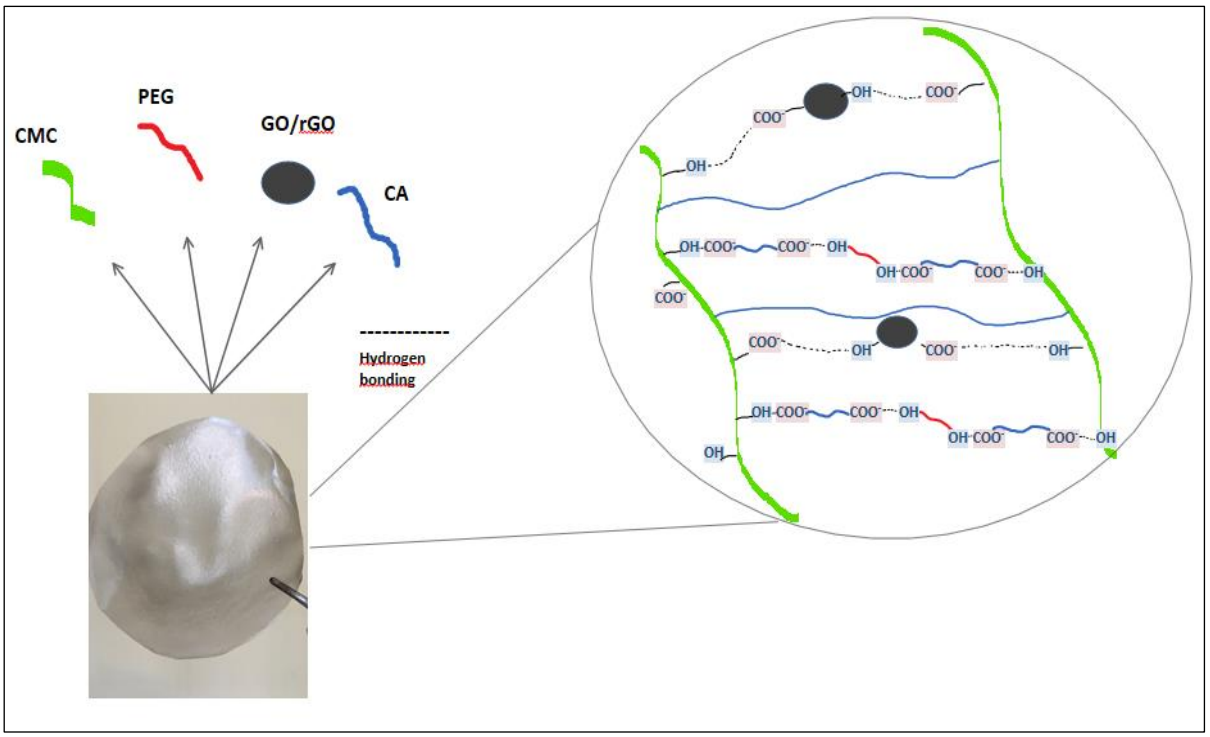

Figure 3.4: Schematic illustration of the GO/rGO containing hydrogel stcructure

3.4. Characterization of CMC Based Conductive Hydrogels

The fabricated pure, GO/rGO reinforced CMC based hydrogels were characterized by FT-IR and SEM analyses.

As seen from Fig. 3.5, the characteristics peaks of CMC, PEG and CA were appeared in the FT-IR spectrum. The peaks at 2877 cm^{-1} and 3357 cm^{-1} demonstrates the C-H and O-H stretching of CMC, PEG and CA [28, 54]. The peaks that observed around 1727 cm^{-1} and 1242 cm^{-1} refer to the C=O and C-O stretching vibrations respectively which represents carboxylic acid groups of CMC and CA. These peaks (C=O, C-O) also confirm the possible crosslinking effect through esterification reaction which comes true between CA and hydroxyl groups of the CMC and PEG [56, 57]. In addition, it can be stated that the peak at 1409 cm^{-1} demonstrates stretching vibrations of COO^- carbonyl groups of CMC [28]. In the spectrum of GO or rGO reinforced hydrogel, beside of these characteristics peaks, the peak that was seen at 1585 cm^{-1} is ascribed to the C=C bond of GO/rGO [47] and the peak that occurs at 1105 cm^{-1} represents the epoxide (C-O-C) groups of GO/rGO [38].

It can be stated that incorporating GO and rGO in pure CMC based hydrogel resulted in changes in FT-IR spectrum. The intensity of the peak demonstrating O-H stretching at around 3357 cm^{-1} in GO reinforced hydrogel is stronger than pure and rGO incorporated hydrogel which confirms the presence of abundant OH groups in GO structure. This peak that represents OH^- groups also confirms the existence of hydrogen bonding in the structure [28]. In the meantime, it was seen that OH- peaks in hydrogels' spectrum are not very intensive. This might be stemming from the esterification reaction which realized owing to OH^- groups [56]. The peak that observed at 2877 cm^{-1} which shows C-H bond and the intensity of this peak weakens in GO reinforced hydrogel when compared to pure hydrogel. The peak that represents C=C stretching band appears as the strongest in GO reinforced hydrogel while it is weaker in rGO reinforced hydrogel comparatively.

In the FTIR spectrum of GO containing hydrogel, the peak around 1727 cm^{-1}, which shows C=O groups of carboxylic acid is much stronger than pure and rGO reinforced samples. When compared to pure and rGO reinforced hydrogels each other, it was seen that this peak in the sample with rGO is more intense than the pure one. As to the GO

reinforced hydrogel, the peak that represents epoxide groups (1020 cm^{-1}) is pretty more significant rather than rGO reinforced hydrogel.

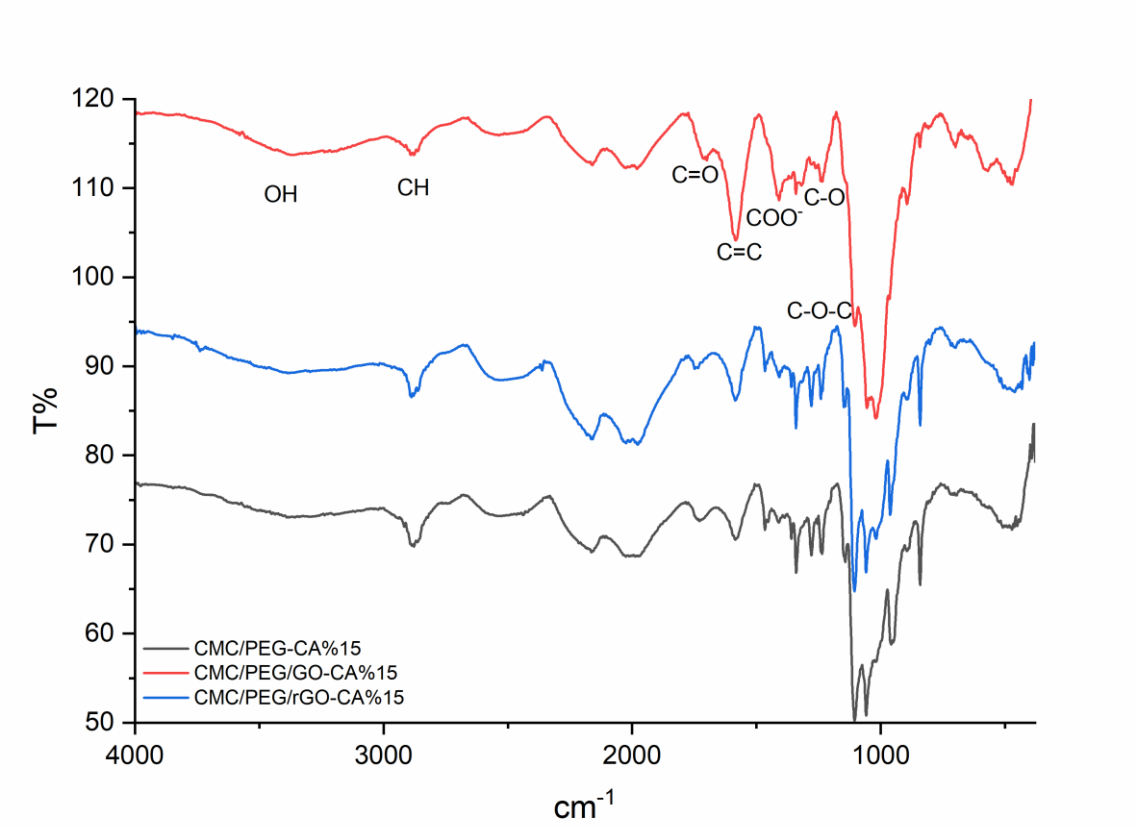

Figure 3.5: FTIR spectrum of the pure, GO and rGO containing hydrogels

3.5. Scanning Electron Microscopy (SEM)

The differences between surface structures of pure, GO reinforced and rGO reinforced hydrogels have been observed by means of SEM images. While the pure film has a smoother structure with no roughness on the surface, GO and rGO reinforced hydrogels have a more roughened surface having hollows and pores thanks to micro-sheet structure of GO or rGO. It should be mentioned that the roughened and porous surface of dressing material helps to wound healing process by providing good attachment to the skin. Furthermore, porous structure acts like a natural extra cellular matrix which supports cell proliferation and attachment [45]. When compared the surface structure of GO and rGO reinforced hydrogel each other, it was seen that while there is a greater separation between individual layers, more porous structure and a highly disordered surface morphology

because of the functional groups that contain oxygen in GO incorporated hydrogel, rGO reinforced hydrogel has a smaller interlayer spacing and more ordered surface morphology owing to restored hexagonal lattice structure resulting from the oxygen removal.

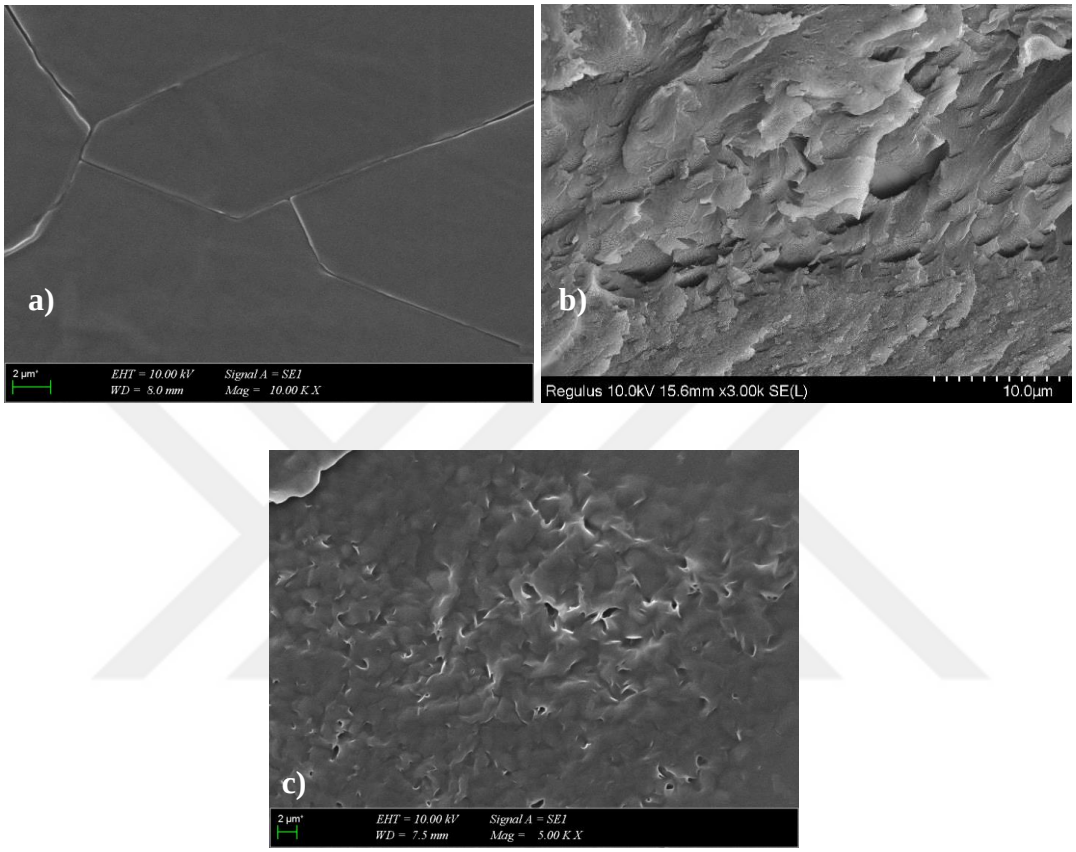

Figure 3.6: SEM figures of the a) CMC/PEG-CA15%, b) CMC/PEG/GO-CA15% and c) CMC/PEG/rGO-CA15%

3.6. Toxicity Results

The toxicity tests carried out using L-929 fibroblast cells by MTT analyses showed that the fabricated hydrogels with different compositions (CMC/PEG-CA15%, CMC/PEG/GO-CA15%, CMC/PEG/rGO-CA15%) have no toxic effect on the cells. Moreover, it observed that the formulations including GO or rGO have more contributed to cell proliferation owing to their functional groups and the formation of surfaces with roughness [31].

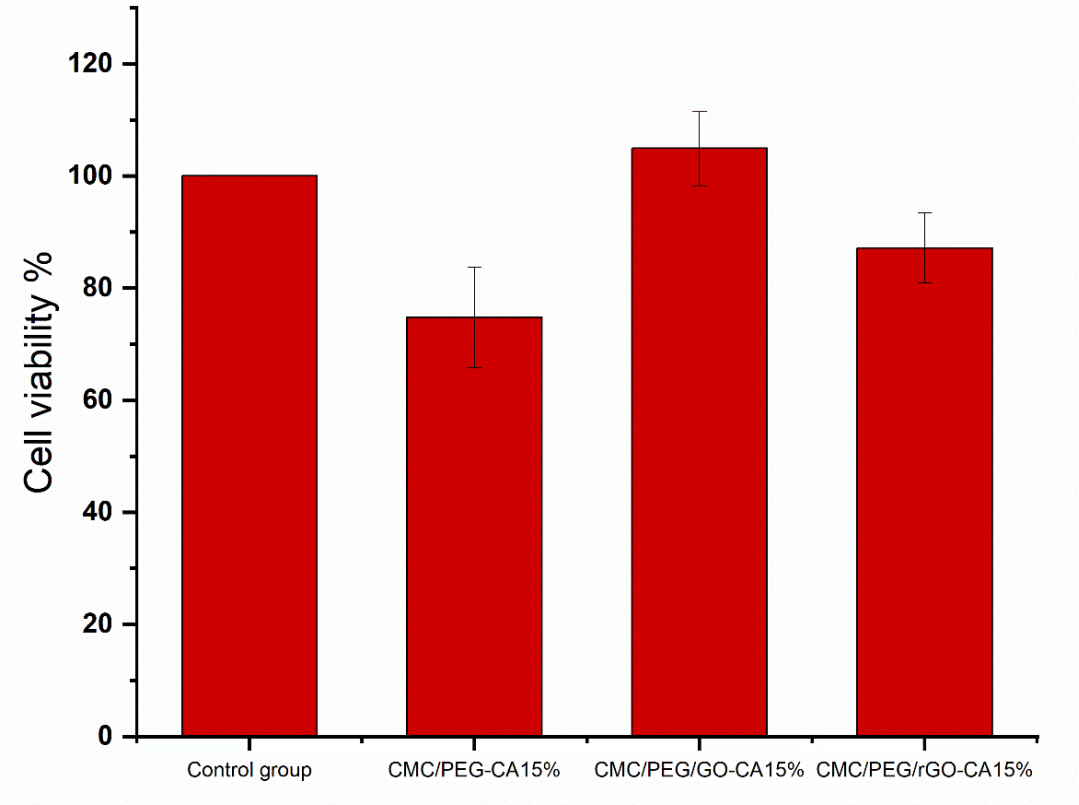

Figure 3.7: Cell viability of the pure, GO and rGO containing hydrogels

3.7. Swelling Studies

Swelling capacity is quite essential for wound dressing materials since a moist environment should be provided at the wound site to promote healing. Therefore, the effects of CA amount, PEG amount, GO and RGO amount in the hydrogels' compositions on the swelling properties of polymeric film were investigated in detail. The obtained results for each parameter were shown as a graph. As seen from figure 3.8, swelling ratio was decreased with the increasing amount of CA which was used as a crosslinker. It can be explained that the more crosslinking density increases, the more extra network occurs in hydrogel which results in a compact structure that does not allow to take in large amounts of water into the hydrogel's structure.

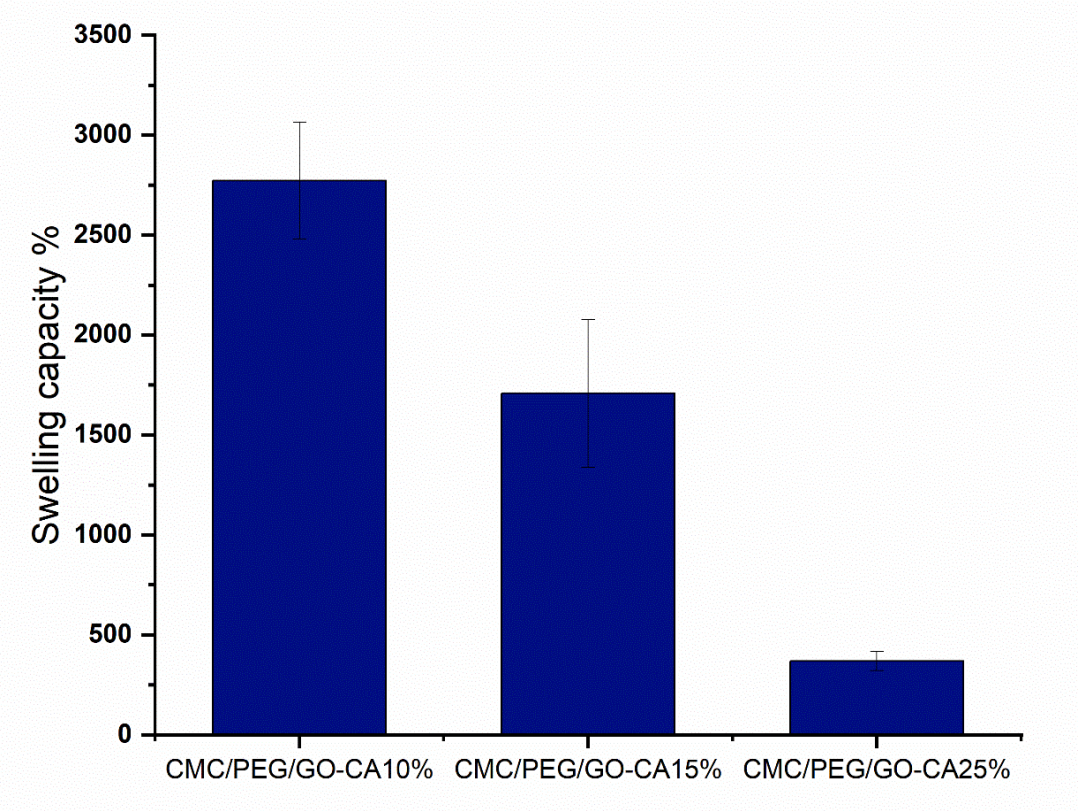

Figure 3.8: The effect of amount of CA on swelling properties

When observed the effect of the amount of PEG on the swelling capacity (Figure 3.9), it was seen that the swelling ratio increased with an increasing PEG amount of up to 50%. However, an excess amount of PEG resulted in a denser network structure eventually blocking the water uptake capacity. This is because, PEG is acting as a crosslinker by improving hydrogel network through intermolecular hydrogen bonding that it forms between the PEG and not only the crosslinker CA but also cellulosic chains of CMC.

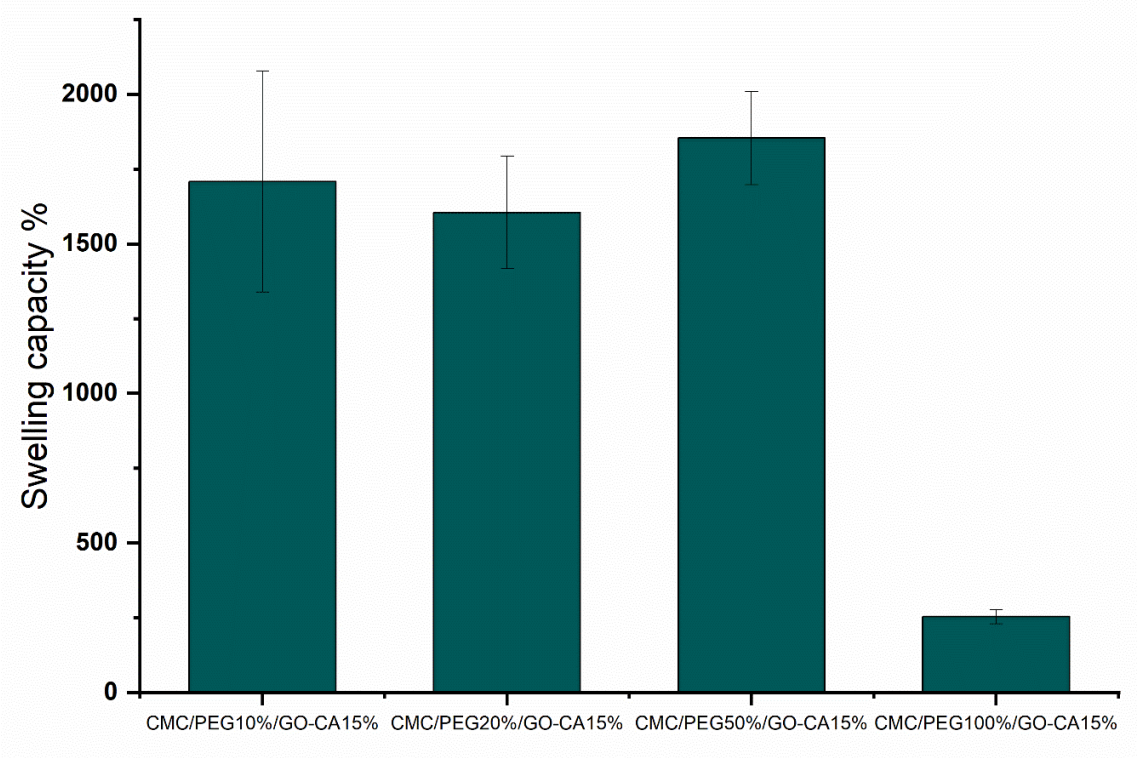

Figure 3.9: The effect of amount of PEG on swelling properties

As seen from the figure 3.10, GO containing hydrogel showed better water uptake capacity (1708%) when compared with pure hydrogel (1312%) and rGO reinforced hydrogel (605%). This result can be associated to the abundant amount of functional groups that contain oxygen (hydroxyl, carboxyl, and epoxide) covalently bonded to GO provide hydrophilicity to the structure, since these groups would allow to attract to water molecules [27]. Additionally, when the graphite layers is oxidated to produce GO, the interplanar distance of the layers increases and thus the gap to take the water into the hydrogel rises. As for, rGO, the amount of functional groups that contain oxygen decrease because of the reduction process which leads to diminishing hydrophilic character of the structure. Additionally, it should be mentioned that the structure of hydrophilic character diminishes due to the increasing of C/O ratio in the structure after the reduction process.

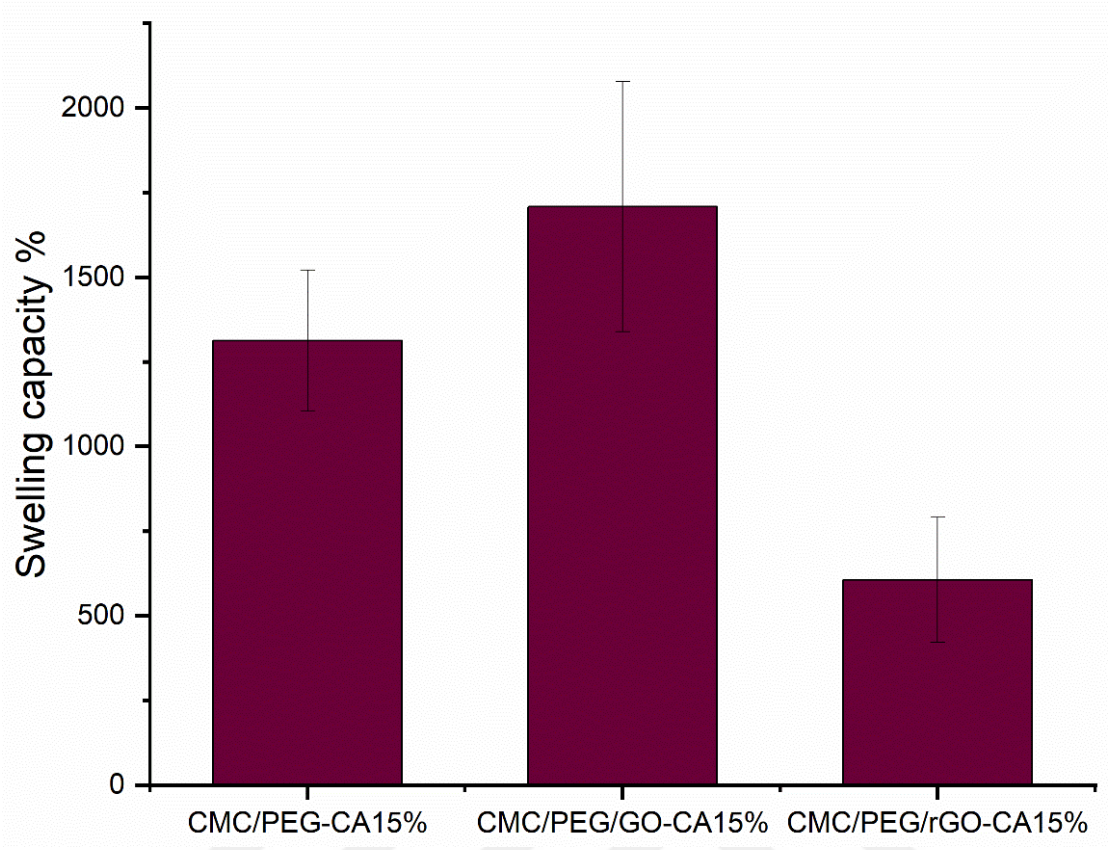

Figure 3.10: Swelling properties of the pure hydrogel, GO reinforced hydrogel and rGO reinforced hydrogel.

According to all swelling ratio results, while the optimum amount of CA and PEG were chosen as 15% (w/w) and 10% (w/w) of CMC amount respectively; the amount of GO and rGO were determined as 0,37% in the CMC-based hydrogel formulation. These samples were represented as CMC/PEG-CA15%, CMC/PEG/GO-CA15% and CMC/PEG/rGO-CA15% and exposed to further analyses such as mechanical tests, water vapor permeability, conductivity and drug release behavior to understand whether the fabricated CMC-based hydrogel fulfills the desired properties of an ideal wound dressing.

3.8. Mechanical Tests

Mechanical performance is quite important parameter for a wound dressing material in terms of various reasons such as providing a stable connection between the wound site and the material, providing a good strength and elasticity so that the wound dressing does not stick to the wound surface or break under high stress [41, 42]. The mechanical properties, (elastic modulus (N/mm^2), tensile strength (MPa) and elongation at break (%)

values) of pure, GO reinforced and rGO reinforced hydrogels have been investigated to comprehend the mechanical reinforcement effect of the GO and rGO to the material's structure. The results showed that, while pure hydrogel has an elastic modulus of 103,9 N/mm^2, GO and rGO reinforced hydrogels have the elastic modulus as 426,19 N/mm^2 and 1010,66 N/mm^2, respectively. Figure 3.12 shows that the highest tensile strength value (87,99 MPa) was also obtained in the case of CMC/PEG/rGO-CA15% hydrogel when compared to CMC/PEG-CA15% (29,62 MPa) and CMC/PEG/GO-CA15% (62,22 MPa). As for the elongation at break values, CMC/PEG/rGO-CA15% showed the best result with 12,95% while CMC/PEG/GO-CA15% and CMC/PEG-CA15% achieved to 5,58 % and 5,73% respectively.

These results are quite evident that both GO and rGO improved the mechanical performance of a pure hydrogel. This prominent reinforcement effect caused by GO or rGO is considered to be due to the strong hydrogen bonding between GO or rGO and the polymeric structure of CMC. This bonding makes stress transfer easier by acting as interfacial load transfer paths [46, 48]. Moreover, GO or rGO's sheet-like structure provides good interfacial interaction [47].

It should be also noted that rGO reinforced hydrogel demonstrated the best mechanical performance among the fabricated materials (GO or rGO-reinforced hydrogel and pure hydrogel). In other words, rGO provided more contribution to the mechanical performance of the material since the elimination of oxygen containing compounds by means of reduction process leads to a higher specific surface which supports the stress to be distributed uniformly through the structure of polymeric material and improves the mechanical properties by increasing the adhesion surface per unit volume. Another important reason behind rGO's stronger mechanical reinforcement effect may be attributed to the fact that defects in the carbon network is restored and interlayer spacing between rGO sheets are reduced due to the reduction of GO [48].

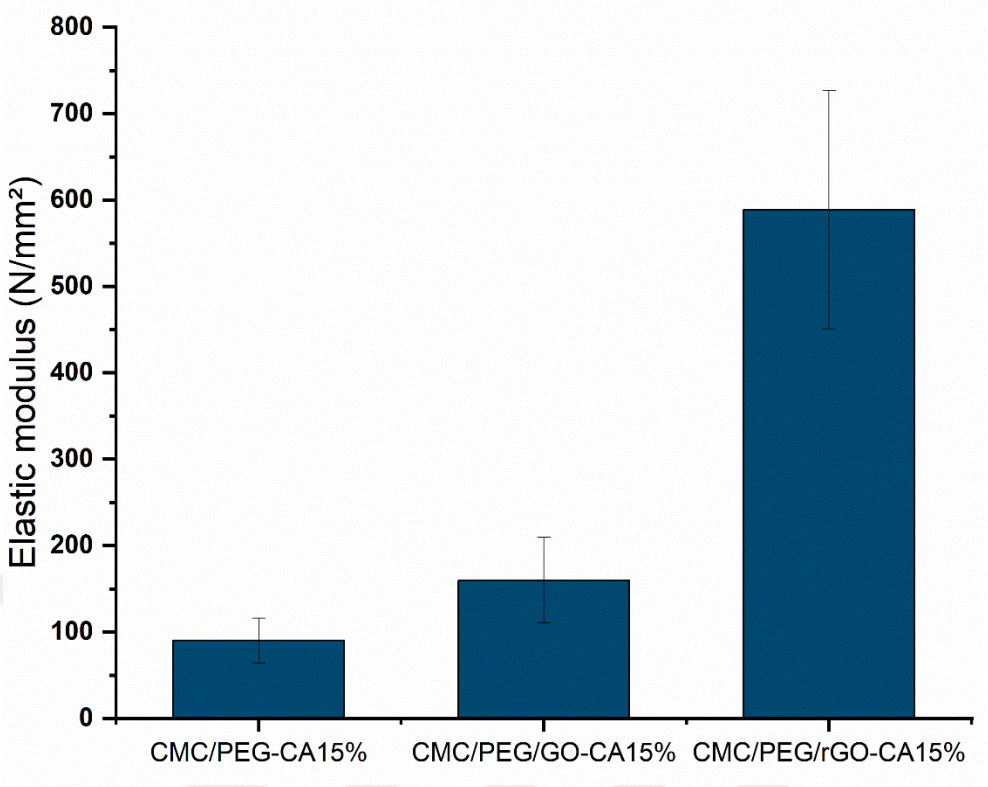

Figure 3.11: Elastic modulus (N/mm^2) of the pure, GO and rGO containing hydrogels

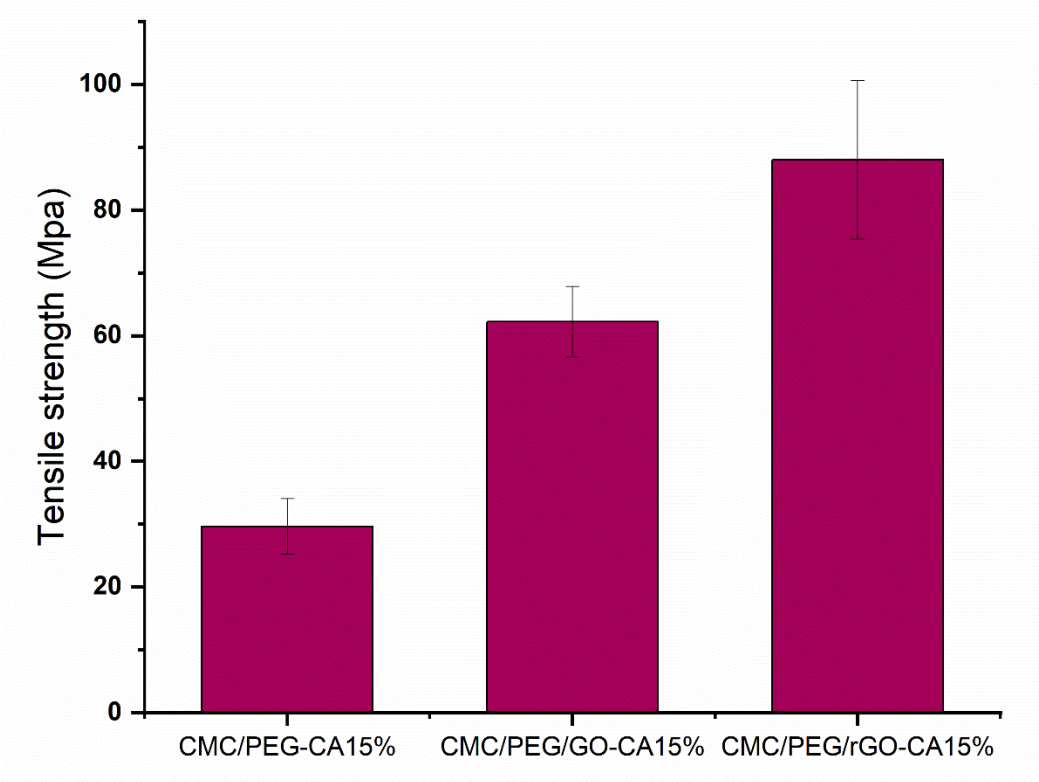

Figure 3.12: Tensile strength (MPa) of the pure, GO and rGO containing hydrogels

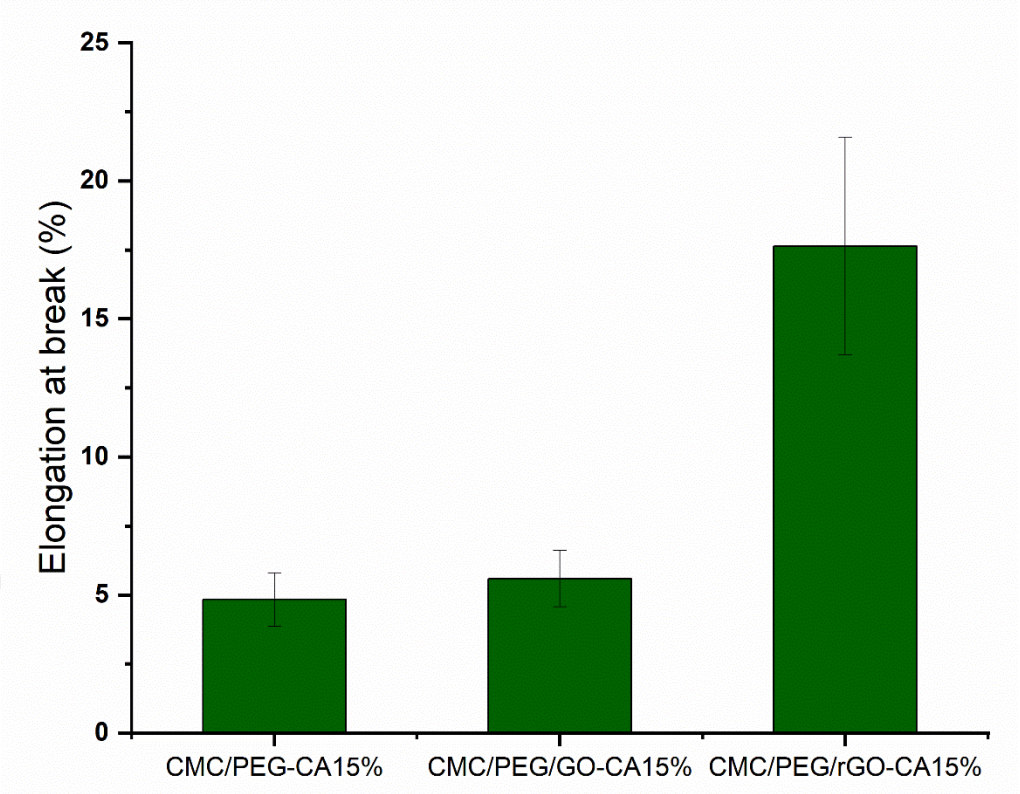

Figure 3.13: Elongation at break (%) of the pure, GO and rGO containing hydrogels

3.9. Water Vapor Permeability

The evaluation of WVP of dressing material is very important feature to ensure a suitable moist environment for the wound healing process. While highly permeable materials for water vapor can cause dehydration at the wound site leading to scar formation, low level WVP may result the wound infection which retards the healing process of wound. WVP of a wound dressing material should be adjusted based on the type of the wound and its exudate amount because moisture needs can change considering these conditions [44].

Table 3.1: Water vapor permeability values of the produced hydrogels

Sample	**WVP*10^{-7} g/Pa.h.m**
CMC/PEG-CA15%	1,5
CMC/PEG/GO-CA15%	1,3
CMC/PEG/rGO-CA15%	1

According to the obtained WVP results that can be seen from the Table 3.1, the dressing material including GO or rGO (CMC/PEG/GO-CA15% and CMC/PEG/rGO-CA15%)

has showed less water vapour permeability when compared to the pure film (CMC/PEG-CA15%). It can be clarified that since the pores of the polymeric film were clogged by the GO and rGO particles which lead to increase in diffusion paths from where water vapor permeates and reduce free volume of polymer matrix. Additionally, the development of new intermolecular bonding especially hydrogen bonding between GO or rGO particles and polymeric structure enhances hydrogel's 3D structure and thus water molecules have to follow more devious permeation path [43].

The low WVP values of CMC/PEG/GO-CA15% and CMC/PEG/rGO-CA15% patches could be considered as an advantage to prevent wound dehydration and provide adequate moisture for healing mechanism [55].

When compared to GO and rGO with each other, the sample including rGO has lower WVP value than GO. This behavior can be explained that there is a two competitive effect in this case of GO. One hand GO is filling the pores of polymeric matrix on the other hand GO has more oxygen containing functional groups and thus more hydrophilic character compared to rGO which improves the WVP of the polymeric film [52].

3.10. Conductivity

Conductive wound dressing materials could be beneficial for wound healing as they can help to the activities of electrically sensitive skin cells. The effect of GO and rGO to conductive properties of hydrogels have been determined by using four-probe method and the obtained results were given in figure 3.14. According to the results, CMC/PEG/rGO-CA15% has reached to a higher conductivity value ($3.01x10^{-6}$ $S.cm^{-1}$) than CMC/PEG/GO-CA15% ($0.85x10^{-6}$ $S.cm^{-1}$) expectedly. There are two important reason i) sp3 hybridized carbon atoms formed in the GO production eliminate the honeycomb lattice structure consisting of sp^2 hybridized carbon atoms. This elimination causes a loss of conductivity, ii) the reduction process carried out for rGO production improves conductivity since it restores the sp^2 hybridized carbon atoms. In other words, sp^2/sp^3 ratio is lower in the GO structure due to the change in the carbon orbitals from sp^2 to sp^3. This disruption of π conjugation leads to decrement of electrical conductivity. Owing to the reduction of GO (rGO), the honeycomb lattice structure is repaired again and better electrical conductivity is achieved [51].

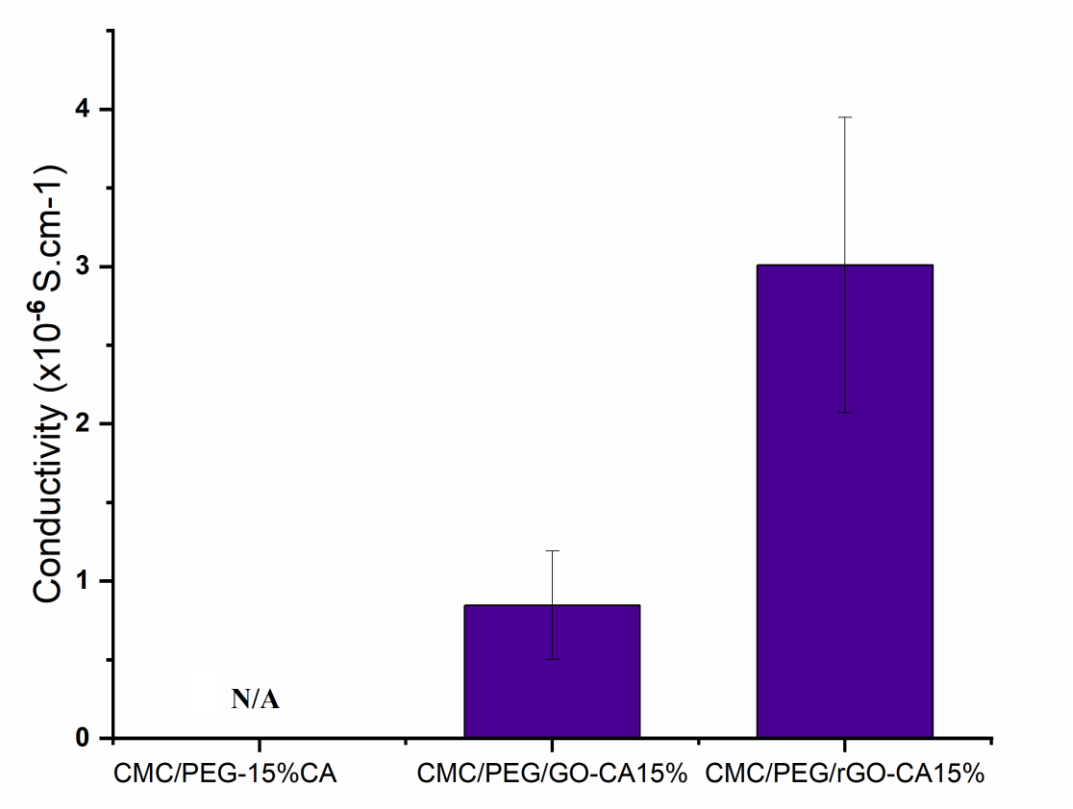

Figure 3.14: Conductivity values of the produced hydrogel samples

3.11. Drug Release

Drug release behavior in wound dressing materials is an important point for wound healing mechanism. Herein, release behaviour of the curcumin from the fabricated wound dressing materials was investigated to understand the effect of GO or rGO on the release kinetic. According to the drug release studies (Figure 3.15), CMC/PEG/rGO-CA15% has demonstrated the least burst release among produced materials which is an important feature for a controlled release system because drug overdose and toxicity problems may occur in early burst release stage. As confirmed by the swelling ratio and mechanical performance results, the structure of rGO-reinforced hydrogel has less hydrophilic and more compact structure than pure and GO incorporated hydrogel resulting in the release of curcumin in the more controlled manner.

Ideally, a slow release over a few days after burst release to some extent can provide a suitable curing period [49]. When compared to rGO, pure and GO reinforced hydrogel have the higher swelling ratios which allow the easier diffusion of the drug molecules and thus leads to faster drug release rates.

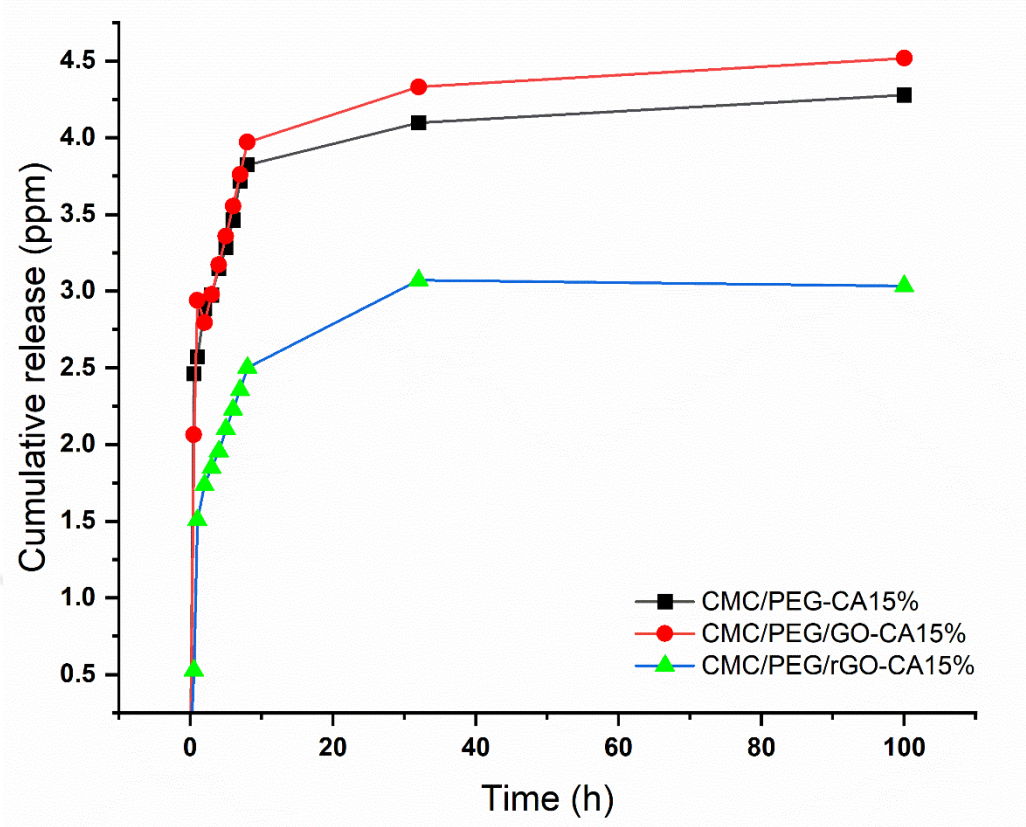

Figure 3.15: Drug release behavior of the produced hydrogel samples

4. CONCLUSION

Wound healing is an attractive and ongoing research area that comes into question because today many people suffer from skin damage, burn or chronic wounds (diabetic ulcers, pressure ulcers etc) which could have vital results due to infection risk. Modern wound dressing materials with specific properties for wound types are significantly required. To this end, not only wound dressing materials that consist of Carboxymethyl Cellulose (CMC), Polyethylene glycol (PEG) and Graphene Oxide (GO) / Reduced Graphene Oxide (rGO) have been produced but also their special properties (mechanical, conductive, swelling, drug release, cytotoxicity and water vapor permeability) have been investigated and compared to each other in terms of wound dressing performance in this study. While CMC and PEG utilized for polymeric structure and gelation, GO and rGO were employed in order to boost mechanical and electrical properties of the fabricated wound dressing material. It is worthwhile to mention that the synthesis of the used rGO in this thesis has been realized with plant extract (Laurus nobilis) which is an environmentally friendly and less hazardous alternative to use in wound dressing applications. According to the test evaluations, while reinforcing the structure with GO has caused higher swelling ratio (1708%) due to its hydrophilic nature, incorporation of rGO has caused a decrease in water uptake capacity (605%) because of its more compact structure when compared to the pure hydrogel (1312%). The produced hydrogels have exhibited non-toxic results which are above 70% viability and demonstrated good biocompatibility. It is also remarkable in this study that GO reinforced hydrogel has demonstrated a viability ratio up to 104.91% which shows its contribution to cell proliferation. It was observed that addition of GO and rGO has resulted in decrement of WVP ($1.3x10^{-7}$ g/Pa.h.m and $1x10^{-7}$ g/Pa.h.m respectively) as compared to pure hydrogel ($1.5x10^{-7}$ g/Pa.h.m). As for mechanical tests, GO and rGO have substantially contributed to the mechanical features of the hydrogels. The best results for elastic modulus (588.62 N/mm^2), tensile strength (87.99 MPa) and elongation at break (17.64%) values have been achieved by rGO reinforced hydrogel (CMC/PEG/rGO-CA15%). Furthermore, boosting effect of the rGO for electrical conductivity ($3.01x10^{-6}$ $S.cm^{-1}$) has also been proved when compared to GO containing hydrogel ($0.85x10^{-6}$ $S.cm^{-1}$). Drug release behavior of the produced materials has also been analyzed by using curcumin as a model drug and the

results showed the beneficial effect of rGO on the prolonged drug release behavior when compared to GO containing and pure hydrogel.

In conclusion, the produced CMC based hydrogels that contain GO and rGO may be bright candidates to be employed as wound dressing materials. It should be noted that although CMC based hydrogels have been studied in wound dressing applications there is no any study about the comparison of the contribution of GO and rGO to the certain properties of CMC based hydrogel in the literature. Moreover, antibiotic free examination was carried out by using curcumin for the first time in this thesis for wound dressing research area.

REFERENCES

[1] Rezvani Ghomi, E., Khalili, S., Nouri Khorasani, S., Esmaeely Neisiany, R., & Ramakrishna, S. (2019). Wound dressings: Current advances and future directions. Journal of Applied Polymer Science, 136(27), 47738.

[2] Li, H., Williams, G. R., Wu, J., Lv, Y., Sun, X., Wu, H., & Zhu, L. M. (2017). Thermosensitive nanofibers loaded with ciprofloxacin as antibacterial wound dressing materials. International Journal of pharmaceutics, 517(1-2), 135-147.

[3] Jayakumar, R., Prabaharan, M., Kumar, P. S., Nair, S. V., & Tamura, H. (2011). Biomaterials based on chitin and chitosan in wound dressing applications. Biotechnology advances, 29(3), 322-337.

[4] Kim, Y., Doh, S. J., Lee, G. D., Kim, C., & Im, J. N. (2019). Composite nonwovens based on carboxymethyl cellulose for wound dressing materials. Fibers and Polymers, 20(10), 2048-2056.

[5] Simões, D., Miguel, S. P., Ribeiro, M. P., Coutinho, P., Mendonça, A. G., & Correia, I. J. (2018). Recent advances on antimicrobial wound dressing: A review. European Journal of Pharmaceutics and Biopharmaceutics, 127, 130-141.

[6] Kamoun, E. A., Kenawy, E. R. S., & Chen, X. (2017). A review on polymeric hydrogel membranes for wound dressing applications: PVA-based hydrogel dressings. Journal of advanced research, 8(3), 217-233.

[7] Tavakoli, S., & Klar, A. S. (2020). Advanced hydrogels as wound dressings. Biomolecules, 10(8), 1169.

[8] Gupta, A., Kowalczuk, M., Heaselgrave, W., Britland, S. T., Martin, C., & Radecka, I. (2019). The production and application of hydrogels for wound management: A review. European Polymer Journal, 111, 134-151.

[9] Sahana, T. G., & Rekha, P. D. (2018). Biopolymers: Applications in wound healing and skin tissue engineering. Molecular biology reports, 45(6), 2857-2867.

[10] Shi, C., Wang, C., Liu, H., Li, Q., Li, R., Zhang, Y., ... & Wang, J. (2020). Selection of appropriate wound dressing for various wounds. Frontiers in bioengineering and biotechnology, 8, 182.

[11] Das, N. (2013). Preparation methods and properties of hydrogel: A review. Int. J. Pharm. Pharm. Sci, 5(3), 112-117.

[12] Deepachitra, R., Lakshmi, R. P., Sivaranjani, K., Chandra, J. H., & Sastry, T. P. (2015). Nanoparticles embedded biomaterials in wound treatment: a review. J. Chem. Pharm. Sci, 8, 324-329.

[13] Maitra, J., & Shukla, V. K. (2014). Cross-linking in hydrogels-a review. Am. J. Polym. Sci, 4(2), 25-31.

[14] Bashir, S., Hina, M., Iqbal, J., Rajpar, A. H., Mujtaba, M. A., Alghamdi, N. A., ... & Ramesh, S. (2020). Fundamental concepts of hydrogels: Synthesis, properties, and their applications. Polymers, 12(11), 2702.

[15] Alvarez, G. S., Hélary, C., Mebert, A. M., Wang, X., Coradin, T., & Desimone, M. F. (2014). Antibiotic-loaded silica nanoparticle–collagen composite hydrogels with prolonged antimicrobial activity for wound infection prevention. Journal of Materials Chemistry B, 2(29), 4660-4670.

[16] Barroso, A., Mestre, H., Ascenso, A., Simões, S., & Reis, C. (2020). Nanomaterials in wound healing: From material sciences to wound healing applications. Nano Select, 1(5), 443-460.

[17] Ali, N. H., Amin, M. C. I. M., & Ng, S. F. (2019). Sodium carboxymethyl cellulose hydrogels containing reduced graphene oxide (rGO) as a functional antibiofilm wound dressing. Journal of Biomaterials Science, Polymer Edition, 30(8), 629-645.

[18] Mir, M., Ali, M. N., Barakullah, A., Gulzar, A., Arshad, M., Fatima, S., & Asad, M. (2018). Synthetic polymeric biomaterials for wound healing: a review. Progress in biomaterials, 7(1), 1-21.

[19] Rani, M. S. A., Rudhziah, S., Ahmad, A., & Mohamed, N. S. (2014). Biopolymer electrolyte based on derivatives of cellulose from kenaf bast fiber. Polymers, 6(9), 2371-2385.

[20] Farjadian, F., Abbaspour, S., Sadatlu, M. A. A., Mirkiani, S., Ghasemi, A., Hoseini-Ghahfarokhi, M., ... & Hamblin, M. R. (2020). Recent developments in graphene and graphene oxide: Properties, synthesis, and modifications: A review. ChemistrySelect, 5(33), 10200-10219.

[21] Gerani, K., Mortaheb, H. R., & Mokhtarani, B. (2017). Enhancement in performance of sulfonated PES cation-exchange membrane by introducing pristine and sulfonated graphene oxide nanosheets synthesized through hummers and staudenmaier methods. Polymer-Plastics Technology and Engineering, 56(5), 543-555.

[22] He, J., Shi, M., Liang, Y., & Guo, B. (2020). Conductive adhesive self-healing nanocomposite hydrogel wound dressing for photothermal therapy of infected full-thickness skin wounds. Chemical Engineering Journal, 394, 124888.

[23] Ray, S. C. (2015). Application and uses of graphene oxide and reduced graphene oxide. Applications of graphene and graphene-oxide based nanomaterials, 1.

[24] Tarcan, R., Todor-Boer, O., Petrovai, I., Leordean, C., Astilean, S., & Botiz, I. (2020). Reduced graphene oxide today. Journal of Materials Chemistry C, 8(4), 1198-1224.

[25] De Silva, K. K. H., Huang, H. H., Joshi, R. K., & Yoshimura, M. (2017). Chemical reduction of graphene oxide using green reductants. Carbon, 119, 190-199.

[26] Barua, S., Thakur, S., Aidew, L., Buragohain, A. K., Chattopadhyay, P., & Karak, N. (2014). One step preparation of a biocompatible, antimicrobial reduced graphene oxide–silver nanohybrid as a topical antimicrobial agent. RSC Advances, 4(19), 9777-9783.

[27] Junaidi, N. F. D., Khalil, N. A., Jahari, A. F., Shaari, N. Z. K., Shahruddin, M. Z., Alias, N. H., & Othman, N. H. (2018). Effect of graphene oxide (GO) on the surface morphology & hydrophilicity of polyethersulfone (pes). In IOP Conference Series: Materials Science and Engineering, 358, 012047. IOP Publishing.

[28] Capanema, N. S., Mansur, A. A., de Jesus, A. C., Carvalho, S. M., de Oliveira, L. C., & Mansur, H. S. (2018). Superabsorbent crosslinked carboxymethyl cellulose-PEG hydrogels for potential wound dressing applications. International journal of biological macromolecules, 106, 1218-1234.

[29] Ansari, M. Z., Lone, M. N., Sajid, S., & SIddIqUI, W. A. (2018). Novel green synthesis of graphene layers using zante currants and graphene oxide. Oriental Journal of Chemistry, 34(6), 2832.

[30] Zia, K. M., Zuber, M., & Muhammad, A. (Eds.). (2017). Algae based polymers, blends, and composites: chemistry, biotechnology and materials science. Elsevier.

[31] Zhao, R., Li, X., Sun, B., Zhang, Y., Zhang, D., Tang, Z., ... & Wang, C. (2014). Electrospun chitosan/sericin composite nanofibers with antibacterial property as potential wound dressings. International journal of biological macromolecules, 68, 92-97.

[32] Musso, Y. S., Salgado, P. R., & Mauri, A. N. (2017). Smart edible films based on gelatin and curcumin. Food hydrocolloids, 66, 8-15.

[33] Waremra, R. S., & Betaubun, P. (2018). Analysis of electrical properties using the four point probe method. In E3S Web of Conferences (Vol. 73, p. 13019). EDP Sciences.

[34] Alven, S., Nqoro, X., & Aderibigbe, B. A. (2020). Polymer-based materials loaded with curcumin for wound healing applications. Polymers, 12(10), 2286.

[35] Zhao, X., Wu, H., Guo, B., Dong, R., Qiu, Y., & Ma, P. X. (2017). Antibacterial anti-oxidant electroactive injectable hydrogel as self-healing wound dressing with hemostasis and adhesiveness for cutaneous wound healing. Biomaterials, 122, 34-47.

[36] Talikowska, M., Fu, X., & Lisak, G. (2019). Application of conducting polymers to wound care and skin tissue engineering: A review. Biosensors and Bioelectronics, 135, 50-63.

[37] Liang, Y., Zhao, X., Hu, T., Han, Y., & Guo, B. (2019). Mussel-inspired, antibacterial, conductive, antioxidant, injectable composite hydrogel wound dressing to promote the regeneration of infected skin. Journal of colloid and interface science, 556, 514-528.

[38] Lee, D. W., De Los Santos V, L., Seo, J. W., Felix, L. L., Bustamante D, A., Cole, J. M., & Barnes, C. H. W. (2010). The structure of graphite oxide: investigation of its surface chemical groups. The Journal of Physical Chemistry B, 114(17), 5723-5728.

[39] Shahriary, L., & Athawale, A. A. (2014). Graphene oxide synthesized by using modified hummers approach. Int. J. Renew. Energy Environ. Eng, 2(01), 58-63.

[40] Moosa, A. A., & Jaafar, J. N. (2017). Green reduction of graphene oxide using tea leaves extract with applications to lead ions removal from water. Nanosci Nanotechnol, 7(2), 38-47.

[41] Qu, J., Zhao, X., Liang, Y., Zhang, T., Ma, P. X., & Guo, B. (2018). Antibacterial adhesive injectable hydrogels with rapid self-healing, extensibility and compressibility as wound dressing for joints skin wound healing. Biomaterials, 183, 185-199.

[42] Kokabi, M., Sirousazar, M., & Hassan, Z. M. (2007). PVA–clay nanocomposite hydrogels for wound dressing. European polymer journal, 43(3), 773-781.

[43] Kabiri, R., & Namazi, H. (2014). Nanocrystalline cellulose acetate (NCCA)/graphene oxide (GO) nanocomposites with enhanced mechanical properties and barrier against water vapor. Cellulose, 21(5), 3527-3539.

[44] Negut, I., Dorcioman, G., & Grumezescu, V. (2020). Scaffolds for wound healing applications. Polymers, 12(9), 2010.

[45] Bui, H. T., Chung, O. H., Dela Cruz, J., & Park, J. S. (2014). Fabrication and characterization of electrospun curcumin-loaded polycaprolactone-polyethylene glycol nanofibers for enhanced wound healing. Macromolecular Research, 22(12), 1288-1296.

[46] Layek, R. K., Kundu, A., & Nandi, A. K. (2013). High-performance nanocomposites of sodium carboxymethylcellulose and graphene oxide. Macromolecular Materials and Engineering, 298(11), 1166-1175

[47] Ma, T., Chang, P. R., Zheng, P., & Ma, X. (2013). The composites based on plasticized starch and graphene oxide/reduced graphene oxide. Carbohydrate polymers, 94(1), 63-70.

[48] Phiri, J., Johansson, L. S., Gane, P., & Maloney, T. (2018). A comparative study of mechanical, thermal and electrical properties of graphene-, graphene oxide-and reduced graphene oxide-doped microfibrillated cellulose nanocomposites. Composites Part B: Engineering, 147, 104-113.

[49] Elsner, J. J., Berdicevsky, I., & Zilberman, M. (2011). In vitro microbial inhibition and cellular response to novel biodegradable composite wound dressings with controlled release of antibiotics. Acta biomaterialia, 7(1), 325-336.

[50] Mahmoud, A. E. D. (2020). Eco-friendly reduction of graphene oxide via agricultural byproducts or aquatic macrophytes. Materials Chemistry and Physics, 253, 123336.

[51] Ulutürk, C., & Alemdar, N. (2019). Production of reduced graphene oxide-based electrically conductive hydrogel by using modified chitosan. Journal of Applied Polymer Science, 136(40), 48008.

[52] Akter, N., Khan, R. A., Tuhin, M. O., Haque, M. E., Nurnabi, M., Parvin, F., & Islam, R. (2014). Thermomechanical, barrier, and morphological properties of chitosan-reinforced starch-based biodegradable composite films. Journal of Thermoplastic Composite Materials, 27(7), 933-948.

[53] Anagha, B., George, D., Maheswari, P. U., & Begum, K. M. (2019). Biomass derived antimicrobial hybrid cellulose hydrogel with green ZnO nanoparticles for curcumin delivery and its kinetic modelling. Journal of Polymers and the Environment, 27(9), 2054-2067.

[54] Tohamy, H. A. S., El-Sakhawy, M., & Kamel, S. (2021). Carboxymethyl cellulose-grafted graphene oxide/polyethylene glycol for efficient Ni (II) adsorption. Journal of Polymers and the Environment, 29, 859-870.

[55] Venkataprasanna, K. S., Prakash, J., Vignesh, S., Bharath, G., Venkatesan, M., Banat, F., ... & Venkatasubbu, G. D. (2020). Fabrication of Chitosan/PVA/GO/CuO patch for potential wound healing application. International journal of biological macromolecules, 143, 744-762.

[56] Abou-Yousef, H., & Kamel, S. (2015). High efficiency antimicrobial cellulose-based nanocomposite hydrogels. Journal of Applied Polymer Science, 132(31).

[57] Ghorpade, V. S., Yadav, A. V., Dias, R. J., Mali, K. K., Pargaonkar, S. S., Shinde, P. V., & Dhane, N. S. (2018). Citric acid crosslinked carboxymethylcellulose-poly (ethylene glycol) hydrogel films for delivery of poorly soluble drugs. International journal of biological macromolecules, 118, 783-791.

[58] Isopencu, G., Deleanu, I., Busuioc, C., Oprea, O., Surdu, V. A., Bacalum, M., ... & Stoica-Guzun, A. (2023). Bacterial Cellulose—Carboxymethylcellulose Composite Loaded with Turmeric Extract for Antimicrobial Wound Dressing Applications. International Journal of Molecular Sciences, 24(2), 1719.